Available online at www.sciencedirect.com
ScienceDirect
Journal of Sound and Vibration 320 (2009) 584–616
JOURNAL OF SOUND AND VIBRATION
www.elsevier.com/locate/jsvi

A generalised mathematical model and analysis for integrated multi-channel vibration structure–control interaction systems

J.T. Xing*, Y.P. Xiong, W.G. Price

School of Engineering Sciences, Ship Science, University of Southampton, Southampton SO17 1BJ, England, UK

Received 27 May 2008; received in revised form 4 August 2008; accepted 6 August 2008
Handling Editor: L.G. Tham
Available online 16 September 2008

Abstract

A generalised mathematical model and analysis for integrated multi-channel vibration control–structure interaction systems are developed. The governing equations describing the interactions between a generalised elastic structure and a multi-channel electromagnetic excitation and control system are derived. Based on these equations, the stability and dynamic response of the system are analysed. The introduction of an additional dynamic impedance matrix between structure and control system allows vibration structure–control interaction mechanisms to be investigated. The generalised theory provides a basis to measure exactly the dynamic parameters of the structure negating any influence of the excitation and control system. It also allows the design of a more effective control system taking into account the interactions of the control system with structural motions and vice versa. To illustrate the general formulations developed and their applications, simple one- and two-channel systems are investigated using non-dimensional parameters.

1. Introduction

The control of structural vibrations produced by earthquake, wind, engine, waves or other excitation source can be achieved, for example, by modifying rigidities, masses or damping of the structural system under excitation as well as by producing passive or active counter forces through suitable isolators or actuators [1]. Methods to control structural vibrations have been developed and used successfully. For example, approaches are discussed by Housner et al. [1], which provide a detailed review of such developments, whereas Fuller et al. [2] and Elliott [3] describe more fundamental theories and methods for active control.

The mechanism underlying active vibration control is to use the vibration signal measured from a controlled structure as a feedback signal which is then amplified by a suitably chosen amplifier to drive various actuators to produce counter forces to suppress the vibration level of the structure. A control system is, therefore, a physical system consisting of several units involving, for example, various mechanical, electrical, magnetic or hydraulic physical processes, connected to a structure such that the motion and characteristics of the structure are controlled by the control system and vice versa. The control efficiency is affected by the dynamic motion of

*Corresponding author. Tel.: +44 238 059 6549; fax: +44 238 059 3299.
E-mail address: jtxing@soton.ac.uk (J.T. Xing).

0022-460X/$ - see front matter © 2008 Elsevier Ltd. All rights reserved.
doi:10.1016/j.jsv.2008.08.009

the structure. This phenomenon is referred to as a control–structure interaction (CSI). To design an effective control system or to obtain more accurate structural characteristics unaffected by the measurement and control system, an integrated interdisciplinary knowledge base is required relating to various control systems, flexible structures and their physical coupling mechanisms.

CSI developments mainly focus on problems arising in aerospace engineering and the development of protective systems. These include space station solar tracking controls [4–7], flexible space station freedom attitude or orbit control coupling with attached flexible bodies [8–11] as well as a general study of the dynamics and control of an arbitrary spacecraft with interconnected flexible bodies [12]. Practices in aerospace engineering and protective systems demonstrate benefits occur when well-designed control systems are applied to practical cases. For example, Dyke et al. [13] present studies demonstrating significant improvements in the performance and robustness of a protective system when CSI effects are taken into account. Mohl and Davis [14] discuss a CSI experiment in which the integration of active feedback control in a radar's system-level design is used to reduce mechanical constraints introduced in the original antenna design.

In the vibration control field, it has been widely accepted by theoretical analysis, experimental investigations and practical applications that active feedback controls using displacement, velocity and acceleration parameters can modify the effective mass, damping and stiffness of a mechanical system. The fundamental principle involved in these mechanisms is described by Fuller et al. [2]. Electrical stiffness or damping techniques based on displacement or velocity feedback approaches were adopted in aircraft vibration tests to measure and to adjust the distribution of structural parameters [15] whereas, detailed investigations are presented on active damping [16], adaptive structures [17] and active isolation units [18–21] for different vibration isolation requirements.

Alkhatib and Golnaraghi [22] present a comprehensive critical review of active vibration control techniques with examples from mechanical and civil engineering applications. On the basis of 156 references, they address important issues and provide a detailed guide to the problems arising in the design of an active control system. For example, the authors define and describe "a typical active vibration control system is an integration of mechanical and electronic components in synergistic combination with computer/microprocessor control. The major components of any active vibration control system are the mechanical structure influenced by disturbance, sensors, controllers and actuators." Therefore, to analyse such a system, it is essential to assemble a set of *coupled* equations to describe the dynamics of the rigid or flexible structure, the dynamics of the actuator and the behaviour of the control system. In general, to describe and understand the physical interaction mechanisms of the integrated system, the developed mathematical model must correctly describe the dynamics of each element and the resulting coupled equations cannot be solved separately but in unison. However, as deduced from the details described in the review paper [22], this integrated coupling analysis has not been fully addressed in structure–control interaction systems, because key effects are omitted in the mathematical models. For example, (i) in Eq. (1) of the review paper, the measured output $\mathbf{y}$ depends only on the displacement and velocity of the structure with omission of the effects of the structure's acceleration and actuator dynamics, (ii) in Eq. (23), the feedback control $\mathbf{u} = -\mathbf{G}\mathbf{y}$ is used to investigate the stability of the system to determine a feedback gain matrix $\mathbf{G}$ but the actuator dynamics and the equation describing the behaviour of the control system are not involved, (iii) furthermore, in the Section 17 of the review paper, the actuator–structure interaction is only analysed. Therefore there is no consideration of the equation describing the electrical–magnetic control system, which causes the difference between the feedback force applied to the structure and the force (applied to the coil) produced by an electric–magnetic effect.

Because of these gaps in the review paper [22], the objective of this study is to construct an integrated mathematical model which incorporates mechanical and electrical interaction mechanisms to investigate structure–control interaction systems. To do so, we address this general problem by theoretically investigating a generalised multi-channel vibration CSI system. To replicate vibration tests [23,24], the control system and actuator described in the model are of the electromagnetic type. The paper presents a derivation of the linearised differential equations governing the dynamics of the structure and actuator, the behaviour and characteristics of the electromagnetic control systems and their interactions allowing the formulation and numerical analysis of a set of generalised coupled matrix equations from which the interaction dynamics of the integrated system is derived. In the mathematical model, the variables adopted to describe the mechanical vibrations are displacements, velocities and accelerations, whereas, for the dynamics of the control system and

components (e.g., sensors, power amplifiers, etc.), they are the electric currents and voltages. The stability of the overall system and excited mechanical and electrical responses by external disturbances are analysed. From the developed general mathematical model, by introducing simplifications, selected systems are deduced. To further illustrate applications of the proposed general theory, a single channel system with an electromagnetic actuator or exciter system is chosen and a detailed analysis of its behaviour presented.

2. Governing equations of a multi-channel vibration structure–control interaction system

To examine the interactions between a flexible structure and a multi-channel electromagnetic excitation and control system, Fig. 1 schematically illustrates a possible generalised n-channel control system. The flexible structure represents, for example, an aircraft, ship, simple beam or a component of a large system which experiences excitations. The aim is to control the excited response at various positions on the structure through imposed mechanisms and to understand the effect of one part of the assembled system on another. Fig. 2 shows a flexible structure–single channel control interaction system including details of a proposed electromagnetic exciter. The exciter produces an excitation force applied in a small volume around point A on the structure through a thin rigid rod attached to the moving coil of the exciter. In addition, the positions of excitation and measurement may not necessarily be at the same point. However, in a practical one-channel system, the positions of excitation and measurement are best situated at the point where there is a significant dynamic response to produce accuracy of measurement. Each channel illustrated in Fig. 1 is similar to the one shown in Fig. 2 but also includes inter-connection between channels.

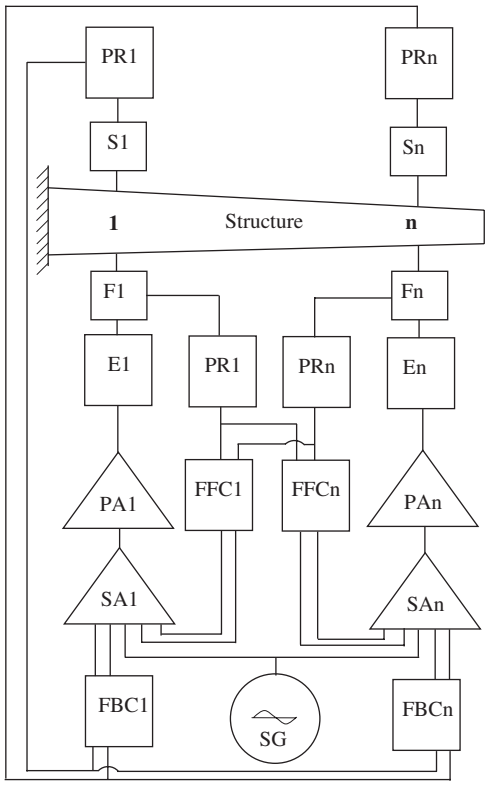

Fig. 1. A typical multi-channel active control–structure interaction system. Notation: subscript α, $\beta(=1,2,3,\ldots,n)$ identify input and measurement locations, SG a signal generator, SA_α a summation amplifier, PA_α a power amplifier, PR_β a pre-amplifier, FFC_β a force feed-forward control unit, FBC_β a displacement, velocity and acceleration feedback control unit, F_β a force transducer, S_β a dynamic response signal transducer, E_α an electromagnetic exciter.

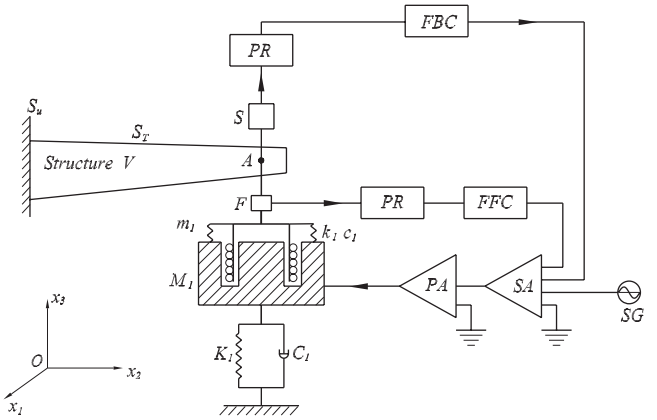

Fig. 2. A single channel (α, $\beta = 1$) active control–structure interaction system in which details of the electromagnetic exciter are shown. Notation: m_α mass of moving part (force transducer F, moving coil and connection rod between structure and exciter) attached to point α on the structure, stiffness coefficient k_α and viscous damping coefficient c_α of a coil supporting unit connected to the magnetic body of the exciter, M_α mass of the magnetic body of the exciter, stiffness coefficient K_α and viscous damping coefficient C_α of the suspension system supporting the exciter.

2.1. Elastic structure

To develop a comprehensive mathematical model of the system shown in Fig. 1, let us assume that the elastic structure occupies domain V with fixed boundary S_u and traction-free boundary S_T. The unit normal vector v_i ($i = 1, 2, 3$) points outwards from the structure. To aid notation, subscripts or superscripts α, β ($= 1, 2, 3, \ldots, n$) identify input and measurement locations, such that the coordinate x_i^β on the structure experiences a measured displacement u_i^β excited by an input sinusoidal force $\tilde{f}_\alpha = \tilde{F}_\alpha e^{j\Omega t}$ of amplitude $\tilde{F}_\alpha$ and frequency Ω produced by the electromagnetic exciter or actuator E_α applied in a small volume $\Delta V_\alpha \neq 0$ around point x_i^α of the structure. The electromagnetic device E_α can act as an exciter and/or actuator. For example, when acting as an exciter, signals from the signal generator SG are its input and therefore it can be considered as a vibration source. As an actuator, feedback signals are inputs, whereas as an exciter and an actuator, signals from both the generator and feedback units are inputs. As normally adopted in mechanics, a positive force is defined as a pulling force applied to the structure. The positive vector γ_i^α defines the direction along the axis of the electromagnetic exciter and towards the excitation point x_i^α. The positive displacement U^α of the magnetic body of the exciter E_α is along the direction γ_i^α. The adoption of traditional notation [25] allows terms such as stress tensor σ_{ij}, displacement vector u_i and velocity vector v_i to retain their usual definitions as well as the complex elastic tensor $E_{ijkl}^* = (1 + j\zeta)E_{ijkl}$, where ζ denotes a hysteretic damping factor describing the structure's material characteristic, which is determined by experiments [26]. In vibration analysis, a viscous damping is normally assumed. However, there are no viscous damping coefficients readily available for structural materials. Therefore, it is usual to assume Rayleigh damping [22] or to calculate an equivalent modal viscous damping coefficient using the hysteretic damping factor ζ and the corresponding mode form of the structure, as described in Appendix A. This paper adopts the latter approach.

The governing equations describing the dynamics of the elastic structure shown in Fig. 1 are defined as follows [25].

Dynamic equation:

$$\sigma_{ij,j} = \rho u_{i,tt} + \sum_{\alpha=1}^{n} \hat{\tilde{f}}_\alpha(\mathbf{x}, \mathbf{x}^\alpha)\gamma_i^\alpha, \quad \mathbf{x} \in V. \tag{1.1}$$

Here, the function $\hat{\tilde{f}}_\alpha(\mathbf{x}, \mathbf{x}^\alpha)$ defines a force distribution function per unit volume around the excitation point $\mathbf{x}^\alpha$ in the form

$$\hat{\tilde{f}}_\alpha(\mathbf{x}, \mathbf{x}^\alpha) = \begin{cases} \tilde{f}_\alpha/\Delta V_\alpha, & \mathbf{x} \in \Delta V_\alpha, \\ 0, & \mathbf{x} \notin \Delta V_\alpha. \end{cases} \tag{1.2}$$

Since the volume $\Delta V_\alpha \neq 0$, as same as for practical cases, for a continuous and differentiable function defined on the body, such as the mode function $\varphi_i^J(\mathbf{x})$ used in this paper, the following volume integration can be obtained by using the mean value theorem for integration as follows:

$$\int_V \varphi_i^J(\mathbf{x})\hat{\tilde{f}}_\alpha(\mathbf{x},\mathbf{x}^\alpha)\gamma_i^\alpha \,\mathrm{d}V = \int_{\Delta V_\alpha} \varphi_i^J(\mathbf{x})\tilde{f}_\alpha/\Delta V_\alpha \gamma_i^\alpha \,\mathrm{d}V = \varphi_i^J(\mathbf{x}_*^\alpha)\tilde{f}_\alpha\gamma_i^\alpha = \phi_{J\alpha}\varphi_i^J(\mathbf{x}^\alpha)\tilde{f}_\alpha\gamma_i^\alpha. \tag{1.3}$$

Here, $\phi_{J\alpha} = [\varphi_i^J(\mathbf{x}_*^\alpha)\gamma_i^\alpha]/[\varphi_i^J(\mathbf{x}^\alpha)\gamma_i^\alpha]$ and $\mathbf{x}_*^\alpha \in \Delta V_\alpha$. It is known that the mode functions of a continuous elastic structure are dependent of by its geometry, mass and stiffness distribution but independent of any external forces applied to it. For the continuous elastic body studied in the paper, all mode functions of the body are well continuous and differentiable with respect to the coordinates. Furthermore, as mentioned earlier, the volume ΔV_α is very small compared with the size of the total structure. Therefore, there should be no obvious difference between the two values at any two points in this small volume ΔV_α of the mode. This supports $\phi_{J\alpha} = 1$ to be chosen for engineering analysis that can reduce much cost without losing required accuracy. However, this general parameter $\phi_{J\alpha}$ is still introduced in following generalised formulations of the mathematical model.

Constitutive equation:

$$\sigma_{ij} = E_{ijkl}^* \varepsilon_{kl}, \quad \mathbf{x} \in V, \tag{2}$$

Geometric relation:

$$\varepsilon_{kl} = \tfrac{1}{2}(u_{k,l} + u_{l,k}), \quad \mathbf{x} \in V, \tag{3}$$

Boundary conditions:

$$\begin{cases} \sigma_{ij} v_j = 0, & \mathbf{x} \in S_T, \\ u_i = 0, & \mathbf{x} \in S_u. \end{cases} \tag{4}$$

It is useful to mention that the governing equation in the tensor form given above cover all types of structures in engineering. Appendix B gives the detailed explanation on it.

2.2. Excitation/control system

2.2.1. Laplace electromagnetic theorem

Let us assume that each electromagnetic exciter E_α obeys the Laplace theorem describing the electromagnetic phenomena [27]. The dynamic current input $i_\alpha(t) = I_\alpha \mathrm{e}^{\mathrm{j}\Omega t}$ into the moving coil of the exciter produces an electromagnetic force $f_\alpha(t) = F_\alpha \mathrm{e}^{\mathrm{j}\Omega t}$ between the moving coil and the outside magnetic body of the exciter as well as an induced voltage $e_\alpha = E_\alpha \mathrm{e}^{\mathrm{j}\Omega t}$ satisfying the relations

$$f_\alpha = i_\alpha B_\alpha \tilde{L}_\alpha = i_\alpha \tilde{B}_\alpha, \tag{5}$$

$$e_\alpha = B_\alpha \tilde{L}_\alpha \tilde{v}_\alpha = \tilde{B}_\alpha \tilde{v}_\alpha. \tag{6}$$

Here B_α represents the intensity of the electromagnetic field in which the coil moves, $\tilde{L}_\alpha$ denotes the effective length of the conductor winding around the moving coil, $\tilde{B}_\alpha = B_\alpha \tilde{L}_\alpha$ and $\tilde{v}_\alpha$ is the velocity of the moving coil relative to the magnetic field. It is assumed that the thin rigid rod connects the moving coil to the position α on the structure. Therefore, the absolute velocity of the moving coil equals the velocity v_i^α at position α and its absolute component along the direction γ_i^α is derived by the scalar product $v_i^\alpha \gamma_i^\alpha$ of the two vectors v_i^α and γ_i^α [25], from which it follows that

$$\tilde{v}_\alpha = v_i^\alpha \gamma_i^\alpha - V_\alpha = \dot{u}_i^\alpha \gamma_i^\alpha - \dot{U}_\alpha. \tag{7}$$

Here $v_i^\alpha = \dot{u}_i^\alpha$ represents the velocity at position α and $V_\alpha = \dot{U}_\alpha$ denotes the velocity in the direction γ_i^α at position α of the magnetic body E_α.

2.2.2. Dynamical and electrical equations of the exciter

By using Newton's law [27], free body diagrams [28,29] and investigating the equilibrium of the latter with inclusion of the effects of moving coil and magnetic body of the exciter [15] as well as using the same notations

for $\alpha = 1$ shown in Fig. 2, we derive the dynamic equations describing the motion of the moving coil with the force transducer F shown in Fig. 2 and the magnetic body of the exciter, respectively, as

$$-\tilde{f}_\alpha + m_\alpha \ddot{u}_i^\alpha \gamma_i^\alpha + c_\alpha(\dot{u}_i^\alpha \gamma_i^\alpha - \dot{U}_\alpha) + k_\alpha(u_i^\alpha \gamma_i^\alpha - U_\alpha) + f_\alpha = 0, \tag{8}$$

$$M_\alpha \ddot{U}_\alpha + C_\alpha \dot{U}_\alpha - c_\alpha(\dot{u}_i^\alpha \gamma_i^\alpha - \dot{U}_\alpha) + K_\alpha U_\alpha - k_\alpha(u_i^\alpha \gamma_i^\alpha - U_\alpha) - f_\alpha = 0. \tag{9}$$

The electric circuit equation of the moving coil takes the form [26]

$$L_\alpha \ddot{Q}_\alpha + R_\alpha \dot{Q}_\alpha + \hat{C}_\alpha^{-1} Q_\alpha + e_\alpha = \tilde{e}_\alpha, \tag{10}$$

where L_α, R_α, $\hat{C}_\alpha$, Q_α and $\tilde{e}_\alpha$ represent the electric inductance, resistance, capacitance, charge and input voltage of the moving coil, respectively, and the electric current $i_\alpha = \dot{Q}_\alpha$. The moving coil acts as a conductor, its capacitance is infinite and therefore Eq. (10) can be represented as

$$L_\alpha \dot{i}_\alpha + R_\alpha i_\alpha + e_\alpha = \tilde{e}_\alpha. \tag{11}$$

2.2.3. Control strategy

Two control strategies are investigated herein. That is, motion feedback and force feed-forward controls [2].

2.2.3.1. Feedback control. In a motion feedback control branch [2], the motion, such as the velocity $v^\beta = v_i^\beta \gamma_i^\beta = \dot{u}_i^\beta \gamma_i^\beta = \dot{u}^\beta$, at position β is measured by a signal transducer S_β which is transferred as an input signal voltage e_s^α to the summation amplifier SA_α through a pre-amplifier PR_β and the feedback control unit FBC_β. This feedback control unit performs an integration and difference operation and can be adjusted to produce the input signal voltage e_s^α, including displacement, velocity and acceleration feedback control, to the summation amplifier SA_α. An application of the method describing feedback control [2] provides an equation representing this feedback process in the form:

$$e_s^\alpha = \sum_{\beta=1}^{n} \left(g_u^{\alpha\beta} u^\beta + g_v^{\alpha\beta} \dot{u}^\beta + g_a^{\alpha\beta} \ddot{u}^\beta\right) H_s^\beta(\Omega), \tag{12}$$

where $g_u^{\alpha\beta}$, $g_v^{\alpha\beta}$ and $g_a^{\alpha\beta}$ denote the feedback gains to channel α from the displacement, velocity and acceleration measured at station β ($= 1, 2, 3, \ldots, n$), respectively, and $H_s^\beta(\Omega)$ describes the transfer function from the signal transducer S_β to the input of the summation amplifier SA_α.

2.2.3.2. Feed-forward control. In a force feed-forward control loop [2], the feed-forward force $\tilde{f}_\beta$ applied at position β on the structure is measured by a force transducer F_β which is transferred as an input signal voltage e_f^α to the summation amplifier SA_α through a pre-amplifier PR_β and the force feedback control unit FFC_β. The equation describing this feed-forward control process [2] is obtained as

$$e_f^\alpha = \sum_{\beta=1}^{n} g_f^{\alpha\beta} \tilde{f}_\beta H_f^\beta(\Omega), \tag{13}$$

where $g_f^{\alpha\beta}$ represents the force feed-forward gain to channel α from the force measured at station β, and $H_f^\beta(\Omega)$ describes the transfer function from the force transducer F_β to the input of the summation amplifier SA_α.

It is assumed that the transfer function of the summation and power amplifiers is represented by $H^\alpha(\Omega)$ and the input voltage of the moving coil of the exciter [23,24] is derived as

$$\tilde{e}_\alpha = (e_s^\alpha + e_f^\alpha + \hat{e}^\alpha) H^\alpha(\Omega), \tag{14}$$

where $\hat{e}^\alpha$ represents a signal voltage input produced by the signal generator SG to the summation amplifier SA_α.

2.3. Combined equations

The substitution of Eqs. (2) and (3) into Eqs. (1) and (4) gives

$$\begin{aligned} &E^*_{ijkl}u_{k,lj} = \rho u_{i,tt} + \sum_{\alpha=1}^{n} \hat{\tilde{f}}_\alpha(\mathbf{x},\mathbf{x}^\alpha)\gamma_i^\alpha, \quad \mathbf{x}\in V,\\ &E^*_{ijkl}u_{k,l}v_j = 0, \quad \mathbf{x}\in S_T,\\ &u_i = 0, \quad \mathbf{x}\in S_u. \end{aligned} \tag{15}$$

These represent the classical displacement equations describing the dynamics of elastic structures. In this equation the force $\hat{\tilde{f}}_\alpha$ applied to the structure is also unknown as well as the unknown displacement u_i. These forces are affected by the characteristics of the control system. Similarly, from Eqs. (5)–(14) the combined equations describing the control system can be rewritten as

$$m_\alpha \ddot{u}^\alpha + c_\alpha \dot{u}^\alpha - c_\alpha \dot{U}_\alpha + k_\alpha u^\alpha - k_\alpha U_\alpha - \tilde{B}_\alpha \dot{Q}_\alpha - \tilde{f}_\alpha = 0, \tag{16}$$

$$M_\alpha \ddot{U}_\alpha + (C_\alpha + c_\alpha)\dot{U}_\alpha - c_\alpha \dot{u}^\alpha + (K_\alpha + k_\alpha)U_\alpha - k_\alpha u^\alpha + \tilde{B}_\alpha \dot{Q}_\alpha = 0, \tag{17}$$

$$\sum_{\beta=1}^{n}(H_a^{\alpha\beta}\ddot{u}^\beta + H_v^{\alpha\beta}\dot{u}^\beta + H_u^{\alpha\beta}u^\beta) + \sum_{\beta=1}^{n} H_f^{\alpha\beta}\tilde{f}_\beta - (L_\alpha \dot{i}_\alpha + R_\alpha i_\alpha) - \tilde{B}_\alpha \dot{u}^\alpha + \tilde{B}_\alpha \dot{U}_\alpha + H^\alpha \hat{e}^\alpha = 0, \tag{18}$$

where

$$\begin{aligned} &H_a^{\alpha\beta} = H^\alpha g_a^{\alpha\beta} H_s^\beta, \quad H_v^{\alpha\beta} = H^\alpha g_v^{\alpha\beta} H_s^\beta,\\ &H_u^{\alpha\beta} = H^\alpha g_u^{\alpha\beta} H_s^\beta, \quad H_f^{\alpha\beta} = H^\alpha g_f^{\alpha\beta} H_f^\beta, \quad u_\alpha = u_i(\mathbf{x}^\alpha)\gamma_i^\alpha. \end{aligned} \tag{19}$$

Eqs. (15)–(19) form a set of governing equations describing the dynamics of the structure–control interaction system. In these coupled equations, the displacement field u_i of the structure, the displacement U_α of the magnetic body of the exciter, the resultant force $\tilde{f}_\alpha$ applied to the structure and the electric current i_α in the moving coil are to be determined.

3. Analysis of control–structure interactions

3.1. Mode transformation and matrix equations

Let us assume that the natural modes and the corresponding natural frequencies of the structure free of any excitation and measurement systems are represented by $\varphi_i^I(\mathbf{x})$ and ω^I ($I = 1,2,3,\ldots$), respectively. These natural modes and frequencies satisfy the orthogonal relationships [26,27]

$$\int_V \varphi_i^I \rho \varphi_i^J \,\mathrm{d}V = \delta_{IJ}\tilde{M}^J, \tag{20}$$

$$\int_V \varphi_{i,j}^I E_{ijkl} \varphi_{k,l}^J \,\mathrm{d}V = \delta_{IJ}\tilde{K}^J, \tag{21}$$

where δ_{IJ} is the Kronecker delta function, $\tilde{M}^J$ and $\tilde{K}^J$ are the generalised mass and stiffness of the Jth mode of the structure, respectively.

For convenience in this analysis, an equivalent viscous damping coefficient $\tilde{C}^J$ of mode J is introduced [30]. This equivalent viscous damping coefficient $\tilde{C}^J$ can be determined by equalling the dissipative energy caused by an equivalent viscous damping in a vibration period of the Jth mode to one dissipated by the material damping in the same vibration period (see Appendix A).

Using the mode superposition method [30], supported by Sturm–Liouville theorem [31], we represent the displacement of the structure in the form

$$u_i = \sum_{I=1}^{\infty} \varphi_i^I q^I, \tag{22}$$

or in a matrix expression

$$u_i = \mathbf{\Phi}_i \mathbf{q}, \quad \mathbf{\Phi}_i = \begin{bmatrix} \varphi_i^1 & \varphi_i^2 & \cdots & \varphi_i^N \end{bmatrix}, \quad \mathbf{q} = \begin{bmatrix} q^1 & q^2 & \cdots & q^N \end{bmatrix}^{\mathrm{T}}, \tag{23}$$

where the first N modes are admitted in the analysis and q^J denotes a time-dependent generalised coordinate requiring determination. The application of the mode transformation described in Eq. (23) in association with the orthogonality relationships defined in Eqs. (20) and (21) as well as the introduction of a viscous damping to replace the original material damping transform the dynamic Eqs. (15)–(19) into the following matrix form:

$$\tilde{\mathbf{M}}\ddot{\mathbf{q}} + \tilde{\mathbf{C}}\dot{\mathbf{q}} + \tilde{\mathbf{K}}\mathbf{q} + \boldsymbol{\theta}\tilde{\mathbf{\Phi}}^{\mathrm{T}}\tilde{\mathbf{f}} = 0, \tag{24}$$

$$\mathbf{m}\tilde{\mathbf{\Phi}}\ddot{\mathbf{q}} + \mathbf{c}\tilde{\mathbf{\Phi}}\dot{\mathbf{q}} + \mathbf{k}\tilde{\mathbf{\Phi}}\mathbf{q} - \mathbf{c}\dot{\mathbf{U}} - \mathbf{k}\mathbf{U} - \tilde{\mathbf{B}}\mathbf{I} - \tilde{\mathbf{f}} = 0, \tag{25}$$

$$-\mathbf{c}\tilde{\mathbf{\Phi}}\dot{\mathbf{q}} - \mathbf{k}\tilde{\mathbf{\Phi}}\mathbf{q} + \mathbf{M}\ddot{\mathbf{U}} + (\mathbf{C}+\mathbf{c})\dot{\mathbf{U}} + (\mathbf{K}+\mathbf{k})\mathbf{U} + \tilde{\mathbf{B}}\mathbf{I} = 0, \tag{26}$$

$$\mathbf{H}_a\tilde{\mathbf{\Phi}}\ddot{\mathbf{q}} + (\mathbf{H}_v - \tilde{\mathbf{B}})\tilde{\mathbf{\Phi}}\dot{\mathbf{q}} + \mathbf{H}_u\tilde{\mathbf{\Phi}}\mathbf{q} + \tilde{\mathbf{B}}\dot{\mathbf{U}} - (\mathbf{L}\dot{\mathbf{I}} + \mathbf{R}\mathbf{I}) + \mathbf{H}_f\tilde{\mathbf{f}} = -\mathbf{H}\hat{\mathbf{e}}, \tag{27}$$

where

$$\tilde{\mathbf{M}} = \mathrm{diag}(\tilde{M}^J), \quad \tilde{\mathbf{C}} = \mathrm{diag}(\tilde{C}^J), \quad \tilde{\mathbf{K}} = \mathrm{diag}(\tilde{K}^J), \tag{28}$$

$$\mathbf{m} = \mathrm{diag}(m_\alpha), \quad \mathbf{c} = \mathrm{diag}(c_\alpha), \quad \mathbf{k} = \mathrm{diag}(k_\alpha), \tag{29}$$

$$\mathbf{M} = \mathrm{diag}(M_\alpha), \quad \mathbf{C} = \mathrm{diag}(C_\alpha), \quad \mathbf{K} = \mathrm{diag}(K_\alpha), \tag{30}$$

$$\mathbf{L} = \mathrm{diag}(L_\alpha), \quad \mathbf{R} = \mathrm{diag}(R_\alpha), \tag{31}$$

$$\mathbf{H} = \mathrm{diag}(H^\alpha), \quad \tilde{\mathbf{B}} = \mathrm{diag}(\tilde{B}_\alpha), \quad \boldsymbol{\theta} = \mathrm{diag}(\phi_{J\alpha}), \tag{32}$$

$$\begin{aligned} &\hat{\mathbf{e}} = \begin{bmatrix} \hat{e}^1 & \hat{e}^2 & \ldots & \hat{e}^n \end{bmatrix}^{\mathrm{T}}, \quad \tilde{\mathbf{f}} = \begin{bmatrix} \tilde{f}_1 & \tilde{f}_2 & \cdots & \tilde{f}_n \end{bmatrix}^{\mathrm{T}}, \\ &\mathbf{U} = \begin{bmatrix} U_1 & U_2 & \ldots & U_\alpha \end{bmatrix}^{\mathrm{T}}, \quad \mathbf{I} = \begin{bmatrix} i_1 & i_2 & \ldots & i_\alpha \end{bmatrix}^{\mathrm{T}}, \end{aligned} \tag{33}$$

$$\tilde{\mathbf{\Phi}}^{\mathrm{T}} = \begin{bmatrix} \boldsymbol{\phi}_1^{\mathrm{T}} & \boldsymbol{\phi}_2^{\mathrm{T}} & \cdots & \boldsymbol{\phi}_n^{\mathrm{T}} \end{bmatrix} = \begin{bmatrix} \varphi^{11} & \varphi^{12} & \ldots & \varphi^{1n} \\ \varphi^{21} & \varphi^{22} & \ldots & \varphi^{2n} \\ \vdots & \vdots & \ddots & \vdots \\ \varphi^{N1} & \varphi^{N2} & \ldots & \varphi^{Nn} \end{bmatrix}, \quad \varphi^{J\alpha} = \varphi_i^J(\mathbf{x}^\alpha)\gamma_i^\alpha, \tag{34}$$

$$\mathbf{H}_b = \begin{bmatrix} H_b^{11} & H_b^{12} & \cdots & H_b^{1n} \\ H_b^{21} & H_b^{22} & \cdots & H_b^{2n} \\ \vdots & \vdots & \ddots & \vdots \\ H_b^{n1} & H_b^{n2} & \cdots & H_b^{nn} \end{bmatrix}, \quad b = a, v, u, f. \tag{35}$$

Eqs. (24)–(27) form a set of matrix coupled equations in which a total of $N+3n$ variables are to be determined. These are the generalised coordinate vector $\mathbf{q}$ (N variables) describing the structure's motion and the three vectors $\mathbf{U}$, $\mathbf{Q}$ and $\tilde{\mathbf{f}}$ each of which is described by n variables defining the motion of the

electromagnetic body, the electric current in the moving coil and the excitation force corresponding to one of the n control channels.

Let us assume that the input signal voltages of all channels are sinusoidal expressed in the matrix form

$$\hat{\mathbf{e}} = \hat{\mathbf{E}}\,\mathrm{e}^{\mathrm{j}\Omega t}, \tag{36}$$

where $\hat{\mathbf{E}}$ represents a vector of the amplitudes of input voltages. Since the system is linear, all mechanical and electrical dynamic responses are sinusoidal quantities with the same frequency. Therefore, these quantities can be represented by

$$\mathbf{q} = \tilde{\mathbf{Q}}\,\mathrm{e}^{\mathrm{j}\Omega t}, \quad \mathbf{U} = \tilde{\mathbf{U}}\,\mathrm{e}^{\mathrm{j}\Omega t}, \quad \mathbf{I} = \tilde{\mathbf{I}}\,\mathrm{e}^{\mathrm{j}\Omega t}, \quad \tilde{\mathbf{f}} = \tilde{\mathbf{F}}\,\mathrm{e}^{\mathrm{j}\Omega t}, \tag{37}$$

where the corresponding amplitude vector of each variable is assumed. Substituting Eqs. (36) and (37) into Eqs. (24)–(27), we obtain an integrated description of the interaction between a vibrating structure and a multi-channel control system as expressed in the following matrix form:

$$\begin{bmatrix} \tilde{\mathbf{Z}} & 0 & 0 & \boldsymbol{\theta}\tilde{\boldsymbol{\Phi}}^{\mathrm{T}} \\ \bar{\mathbf{z}}\tilde{\boldsymbol{\Phi}} & -\mathbf{z} & -\tilde{\mathbf{B}} & -\hat{\mathbf{I}} \\ -\mathbf{z}\tilde{\boldsymbol{\Phi}} & \bar{\mathbf{Z}}+\mathbf{z} & \tilde{\mathbf{B}} & 0 \\ \mathbf{H}^{-1}[\mathrm{j}\Omega\tilde{\mathbf{B}} - \widehat{\mathbf{Z}}\,]\tilde{\boldsymbol{\Phi}} & -\mathrm{j}\Omega\mathbf{H}^{-1}\tilde{\mathbf{B}} & \mathbf{H}^{-1}\mathbf{Z} & -\mathbf{H}^{-1}\mathbf{H}_f \end{bmatrix} \begin{bmatrix} \tilde{\mathbf{Q}} \\ \tilde{\mathbf{U}} \\ \tilde{\mathbf{I}} \\ \tilde{\mathbf{F}} \end{bmatrix} = \begin{bmatrix} 0 \\ 0 \\ 0 \\ \hat{\mathbf{E}} \end{bmatrix}. \tag{38}$$

Here $\hat{\mathbf{I}}$ is a unit matrix of order n and

$$\begin{aligned} &\tilde{\mathbf{Z}} = \tilde{\mathbf{K}} + \mathrm{j}\Omega\tilde{\mathbf{C}} - \Omega^2\tilde{\mathbf{M}}, \quad \bar{\mathbf{Z}} = \mathbf{K} + \mathrm{j}\Omega\mathbf{C} - \Omega^2\mathbf{M}, \quad \mathbf{Z} = \mathbf{R} + \mathrm{j}\Omega\mathbf{L}, \\ &\bar{\mathbf{z}} = \mathbf{z} - \Omega^2\mathbf{m}, \quad \widehat{\mathbf{Z}} = \mathbf{H}_u + \mathrm{j}\Omega\mathbf{H}_v - \Omega^2\mathbf{H}_a, \quad \mathbf{z} = \mathbf{k} + \mathrm{j}\Omega\mathbf{c}, \end{aligned} \tag{39}$$

represent the dynamic modulus (or displacement impedance) matrices of the structure (see, for example, Ref. [26]), the suspension systems of the exciters, the circuits of the moving coils, the moving coils with supporting units, the motion feedback control system and the supporting units of the moving coils, respectively.

3.2. Stability of the coupled system

Eqs. (24)–(27) are a set of linear ordinary differential equations. The stability of these equations is governed by its characteristic equation which is deduced from the determinant of the coefficient matrix of Eq. (38) replacing $\mathrm{j}\Omega$ in Eqs. (38) and (39) by an eigenvalue notation λ [31] and it is expressed in the form

$$D = \begin{vmatrix} \tilde{\mathbf{Z}} & 0 & 0 & \boldsymbol{\theta}\tilde{\boldsymbol{\Phi}}^{\mathrm{T}} \\ \bar{\mathbf{z}}\tilde{\boldsymbol{\Phi}} & -\mathbf{z} & -\tilde{\mathbf{B}} & -\hat{\mathbf{I}} \\ -\mathbf{z}\tilde{\boldsymbol{\Phi}} & \bar{\mathbf{Z}}+\mathbf{z} & \tilde{\mathbf{B}} & 0 \\ \mathbf{H}^{-1}(\lambda\tilde{\mathbf{B}} - \widehat{\mathbf{Z}}\,)\tilde{\boldsymbol{\Phi}} & -\lambda\mathbf{H}^{-1}\tilde{\mathbf{B}} & \mathbf{H}^{-1}\mathbf{Z} & -\mathbf{H}^{-1}\mathbf{H}_f \end{vmatrix} = 0. \tag{40}$$

Stability of the coupled system requires that all eigenvalues λ, denoting the solutions of Eq. (40), have negative real parts. Constructing the Hurwitz determinants and requiring each to have a positive value [32], we can determine the stability of the interacting system.

3.3. Dynamic response of the coupled system

Here the intention is to derive the dynamic response of a stable system subject to the excitation expressed by Eq. (36), where Ω is a real positive frequency as mentioned in Section 2.1. For this stable system, the eigenvalues λ must have negative real parts and therefore, the pure imaginary number $\mathrm{j}\Omega$ is not a solution of Eq. (40). This implies that, in Eq. (38), the coefficient determinant $D \neq 0$ and it follows from Gram's rule [31]

that an unique solution vector is determined by

$$\mathbf{X}_I = \frac{D_I}{D} \quad (I = 1, 2, 3, 4), \tag{41}$$

where $\mathbf{X}_I$ $(I = 1, 2, 3, 4)$ represents the four vectors $\tilde{\mathbf{Q}}$, $\tilde{\mathbf{U}}$, $\tilde{\mathbf{I}}$ and $\tilde{\mathbf{F}}$, respectively, and D_I denotes a determinant with the Ith column of the determinant D replaced by the right-hand side vector of Eq. (38). This solution is substituted into Eq. (26) to obtain the dynamic response of the interactive system.

3.4. Mechanical–electrical–control interactions

To highlight interactions between the mechanical system and the electrical or control system, the elimination of the internal force vector $\tilde{\mathbf{F}}$ applied to the structure by the exciters allows rewriting of Eq. (38) in the form

$$\begin{bmatrix} \tilde{\mathbf{Z}} + \boldsymbol{\theta}\tilde{\boldsymbol{\Phi}}^{\mathrm{T}}\bar{\boldsymbol{z}}\tilde{\boldsymbol{\Phi}} & -\boldsymbol{\theta}\tilde{\boldsymbol{\Phi}}^{\mathrm{T}}\mathbf{z} & -\boldsymbol{\theta}\tilde{\boldsymbol{\Phi}}^{\mathrm{T}}\tilde{\mathbf{B}} \\ -\mathbf{z}\tilde{\boldsymbol{\Phi}} & \bar{\mathbf{Z}} + \mathbf{z} & \tilde{\mathbf{B}} \\ \mathbf{H}^{-1}[\mathrm{j}\Omega\tilde{\mathbf{B}} - \mathbf{H}_f(\bar{\boldsymbol{z}} - \mathbf{z}) - \widehat{\mathbf{Z}}\,]\tilde{\boldsymbol{\Phi}} & -\mathbf{H}^{-1}(\mathbf{H}_f\bar{\mathbf{Z}} + \mathrm{j}\Omega\tilde{\mathbf{B}}) & \mathbf{H}^{-1}\mathbf{Z} \end{bmatrix} \begin{bmatrix} \tilde{\mathbf{Q}} \\ \tilde{\mathbf{U}} \\ \tilde{\mathbf{I}} \end{bmatrix} = \begin{bmatrix} 0 \\ 0 \\ \hat{\mathbf{E}} \end{bmatrix}. \tag{42}$$

From these equations, we deduce an equation describing the motion of the mechanical system influenced by the electrical control units, namely,

$$\begin{aligned} &(\mathbf{Z}_M + \mathbf{Z}_{ME}) \begin{bmatrix} \tilde{\mathbf{Q}} \\ \tilde{\mathbf{U}} \end{bmatrix} = \begin{bmatrix} \boldsymbol{\theta}\tilde{\boldsymbol{\Phi}}^{\mathrm{T}} \\ -\hat{\mathbf{I}} \end{bmatrix} \tilde{\mathbf{B}}\,\mathbf{Z}^{-1}\mathbf{H}\,\hat{\mathbf{E}}, \\ &\mathbf{Z}_M = \begin{bmatrix} \tilde{\mathbf{Z}} + \boldsymbol{\theta}\tilde{\boldsymbol{\Phi}}^{\mathrm{T}}\bar{\boldsymbol{z}}\tilde{\boldsymbol{\Phi}} & -\boldsymbol{\theta}\tilde{\boldsymbol{\Phi}}^{\mathrm{T}}\mathbf{z} \\ -\mathbf{z}\tilde{\boldsymbol{\Phi}} & \bar{\mathbf{Z}} + \mathbf{z} \end{bmatrix}, \\ &\mathbf{Z}_{ME} = \begin{bmatrix} \boldsymbol{\theta}\tilde{\boldsymbol{\Phi}}^{\mathrm{T}}\tilde{\mathbf{B}}\,\mathbf{Z}^{-1}[\mathrm{j}\Omega\tilde{\mathbf{B}} - \mathbf{H}_f(\bar{\boldsymbol{z}} - \mathbf{z}) - \widehat{\mathbf{Z}}\,]\tilde{\boldsymbol{\Phi}} & -\boldsymbol{\theta}\tilde{\boldsymbol{\Phi}}^{\mathrm{T}}\tilde{\mathbf{B}}\,\mathbf{Z}^{-1}(\mathbf{H}_f\bar{\mathbf{Z}} + \mathrm{j}\Omega\tilde{\mathbf{B}}) \\ -\tilde{\mathbf{B}}\,\mathbf{Z}^{-1}[\mathrm{j}\Omega\tilde{\mathbf{B}} - \mathbf{H}_f(\bar{\boldsymbol{z}} - \mathbf{z}) - \widehat{\mathbf{Z}}\,]\tilde{\boldsymbol{\Phi}} & \tilde{\mathbf{B}}\,\mathbf{Z}^{-1}(\mathbf{H}_f\bar{\mathbf{Z}} + \mathrm{j}\Omega\tilde{\mathbf{B}}) \end{bmatrix} \end{aligned} \tag{43}$$

and another equation describing the electrical dynamic equilibrium of the electrical control system influenced by mechanical motions of the structure given by

$$\begin{aligned} &\hat{\mathbf{E}} = (\mathbf{Z}_E + \mathbf{Z}_{EM})\tilde{\mathbf{I}}, \\ &\mathbf{Z}_E = \mathbf{H}^{-1}\mathbf{Z}, \\ &\mathbf{Z}_{EM} = \mathbf{H}^{-1}\Big[\{\mathrm{j}\Omega\tilde{\mathbf{B}} - \mathbf{H}_f(\bar{\boldsymbol{z}} - \mathbf{z}) - \widehat{\mathbf{Z}}\,\}\tilde{\boldsymbol{\Phi}} \quad -(\mathbf{H}_f\bar{\mathbf{Z}} + \mathrm{j}\Omega\tilde{\mathbf{B}})\Big] \begin{bmatrix} \tilde{\mathbf{Z}} + \boldsymbol{\theta}\tilde{\boldsymbol{\Phi}}^{\mathrm{T}}\bar{\boldsymbol{z}}\tilde{\boldsymbol{\Phi}} & -\boldsymbol{\theta}\tilde{\boldsymbol{\Phi}}^{\mathrm{T}}\mathbf{z} \\ -\mathbf{z}\tilde{\boldsymbol{\Phi}} & \bar{\mathbf{Z}} + \mathbf{z} \end{bmatrix}^{-1} \begin{bmatrix} \boldsymbol{\theta}\tilde{\boldsymbol{\Phi}}^{\mathrm{T}}\tilde{\mathbf{B}} \\ -\tilde{\mathbf{B}} \end{bmatrix}. \end{aligned} \tag{44}$$

Here, the inverse matrix can be obtained using the following formulation:

$$\begin{aligned} &\begin{bmatrix} \tilde{\mathbf{Z}} + \boldsymbol{\theta}\tilde{\boldsymbol{\Phi}}^{\mathrm{T}}\bar{\boldsymbol{z}}\tilde{\boldsymbol{\Phi}} & -\boldsymbol{\theta}\tilde{\boldsymbol{\Phi}}^{\mathrm{T}}\mathbf{z} \\ -\mathbf{z}\tilde{\boldsymbol{\Phi}} & \bar{\mathbf{Z}} + \mathbf{z} \end{bmatrix}^{-1} = \begin{bmatrix} \mathbf{G}_{11} & \mathbf{G}_{12} \\ \mathbf{G}_{21} & \mathbf{G}_{22} \end{bmatrix}, \\ &\mathbf{G}_{22} = [\bar{\mathbf{Z}} + \mathbf{z} - \mathbf{z}\tilde{\boldsymbol{\Phi}}(\tilde{\mathbf{Z}} + \boldsymbol{\theta}\tilde{\boldsymbol{\Phi}}^{\mathrm{T}}\bar{\boldsymbol{z}}\tilde{\boldsymbol{\Phi}})^{-1}\boldsymbol{\theta}\tilde{\boldsymbol{\Phi}}^{\mathrm{T}}\mathbf{z}]^{-1}, \quad \mathbf{G}_{12} = (\tilde{\mathbf{Z}} + \boldsymbol{\theta}\tilde{\boldsymbol{\Phi}}^{\mathrm{T}}\bar{\boldsymbol{z}}\tilde{\boldsymbol{\Phi}})^{-1}\boldsymbol{\theta}\tilde{\boldsymbol{\Phi}}^{\mathrm{T}}\mathbf{z}\,\mathbf{G}_{22}, \\ &\mathbf{G}_{21} = \mathbf{G}_{22}\mathbf{z}\tilde{\boldsymbol{\Phi}}\boldsymbol{\theta}(\tilde{\mathbf{Z}} + \tilde{\boldsymbol{\Phi}}^{\mathrm{T}}\bar{\boldsymbol{z}}\tilde{\boldsymbol{\Phi}}\boldsymbol{\theta})^{-1}, \quad \mathbf{G}_{11} = (\tilde{\mathbf{Z}} + \boldsymbol{\theta}\tilde{\boldsymbol{\Phi}}^{\mathrm{T}}\bar{\boldsymbol{z}}\tilde{\boldsymbol{\Phi}})^{-1} + \mathbf{G}_{12}\mathbf{z}\tilde{\boldsymbol{\Phi}}(\tilde{\mathbf{Z}} + \boldsymbol{\theta}\tilde{\boldsymbol{\Phi}}^{\mathrm{T}}\bar{\boldsymbol{z}}\tilde{\boldsymbol{\Phi}})^{-1}. \end{aligned} \tag{45}$$

In Eq. (43), $\mathbf{Z}_M$ represents the dynamic modulus of the mechanical system consisting of the structure and the mechanical parts of the exciters and $\mathbf{Z}_{ME}$ denotes an additional dynamic modulus to the mechanical system due to the electrical control effects in the integrated interaction system. Similarly, in Eq. (44), $\mathbf{Z}_E$ represents the electrical modulus of the excitation-control system consisting of the electrical equipment and

active control units whereas $\mathbf{Z}_{EM}$ provides an additional modulus to the electrical control system arising from the motions of the mechanical system.

The mathematical model and equations together with the solution procedure developed in this section present a generalised theory to analyse a complex structure–control interaction system. The following examples of a single channel system and a vibration test involving a more complex system illustrate aspects of this generalised theory.

4. A single channel system

Fig. 2 represents a system of a single control and excitation channel in which the power amplifier and signal measuring circuit have good direct current characteristics with transfer functions given by $H^1(\Omega)=1$, $H_s^1(\Omega)=1$ and $H_f^1(\Omega)=1$, as required by normal vibration test equipment [15]. To understand more clearly the interaction mechanism, we assume that the structure is modelled by a one degree of freedom system of natural frequency ω_s which equals the frequency of the first mode of the structure and the parameter $\phi_{11}=1$ defined in Eq. (1.3). To simplify description, we neglect sub-, super- and index "1" of the variables used in Fig. 2 and in the equations presented in Section 3, so that the variables defined in Eqs. (28)–(35) and (37) are simplified to

$$\begin{aligned}
&\tilde{\mathbf{Z}}=\tilde{Z}=\tilde{K}+\mathrm{j}\Omega\tilde{C}-\Omega^2\tilde{M},\quad \bar{\mathbf{Z}}=\bar{Z}=K+\mathrm{j}\Omega C-\Omega^2M,\quad \mathbf{Z}=Z=R+\mathrm{j}\Omega L,\\
&\bar{\mathbf{z}}=\bar{z}=k+\mathrm{j}\Omega c-\Omega^2m,\quad \widehat{\mathbf{Z}}=\widehat{Z}=g_u+\mathrm{j}\Omega g_v-\Omega^2g_a,\quad \mathbf{z}=z=k+\mathrm{j}\Omega c,\quad \mathbf{H}=H=1,\\
&\mathbf{H}_u=H_u=g_u,\quad \mathbf{H}_v=H_v=g_v,\quad \mathbf{H}_a=H_a=g_a,\quad \mathbf{H}_f=H_f=g_f,\quad \tilde{\mathbf{\Phi}}=1.
\end{aligned}\tag{46}$$

Eqs. (38) and (42) now take the forms

$$\begin{bmatrix} \tilde{Z} & 0 & 0 & 1\\ \bar{z} & -z & -\tilde{B} & -1\\ -z & \bar{Z}+z & \tilde{B} & 0\\ \mathrm{j}\Omega\tilde{B}-\widehat{Z} & -\mathrm{j}\Omega\tilde{B} & Z & -g_f \end{bmatrix}\begin{bmatrix} u\\ U\\ i\\ \tilde{F}\end{bmatrix}=\begin{bmatrix}0\\0\\0\\ \hat{E}\end{bmatrix},\tag{47}$$

and

$$\begin{bmatrix} \tilde{Z}+\bar{z} & -z & -\tilde{B}\\ -z & \bar{Z}+z & \tilde{B}\\ \mathrm{j}\Omega\tilde{B}+g_f\tilde{Z}-\widehat{Z} & -\mathrm{j}\Omega\tilde{B} & Z \end{bmatrix}\begin{bmatrix} u\\ U\\ i\end{bmatrix}=\begin{bmatrix}0\\0\\ \hat{E}\end{bmatrix},\tag{48}$$

respectively.

For discussion purposes, it is convenient to express these equations in a non-dimensional form. To do so, we define a standard displacement u_0 and electric current i_0 as

$$u_0=\tilde{M}g/\tilde{K},\quad i_0=\hat{E}/R,\tag{49}$$

as well as introducing the following non-dimensional parameters

$$\begin{aligned}
&\psi=\frac{\tilde{B}\hat{E}}{R\tilde{M}g}=\frac{\tilde{B}i_0}{\tilde{M}g},\quad \varepsilon_a\zeta_s=\frac{\tilde{B}g}{2\omega_s\hat{E}}=\frac{\tilde{B}g\omega_s^{-1}}{2\hat{E}},\\
&\eta_s=\Omega/\omega_s,\quad \omega_s=\sqrt{\tilde{K}/\tilde{M}},\quad \zeta_s=\frac{\tilde{C}}{2\tilde{M}\omega_s},\\
&\kappa_c=k/\tilde{K},\quad \varepsilon_c=c/\tilde{C},\quad \mu_c=m/\tilde{M},\quad \varepsilon_e\zeta_s=\frac{L\omega_s}{2R},\\
&\kappa_m=K/\tilde{K},\quad \varepsilon_m=C/\tilde{C},\quad \mu_m=M/\tilde{M},\\
&\kappa_g=\tilde{M}gg_u/(\tilde{K}\hat{E}),\quad \varepsilon_g=\tilde{M}gg_v/(\tilde{C}\hat{E}),\quad \mu_g=gg_a/\hat{E},\quad f_g=\tilde{M}gg_f/\hat{E}.
\end{aligned}\tag{50}$$

Physically, u_0 and i_0 represent the static displacement of the structure subject to its gravitational force $\tilde{M}g$ and the static electric current of the coil conditional on a prescribed electric potential $\hat{E}$. The non-dimensional parameter ψ denotes the ratio of an electromagnetic force $\tilde{B}i_0$ to the gravitational force $\tilde{M}g$ and ε_a is the ratio of the non-dimensional damping $\tilde{B}g\omega_s^{-1}/(2\hat{E})$ caused by the induced voltage of the exciter to the structure's damping ζ_s. These two non-dimensional quantities ψ and ε_a are the characteristic parameters describing mechanical–electric interactions. The other non-dimensional parameters in Eq. (50) have their usual meanings [29].

Pre-multiplying both sides of the resultant non-dimensional Eq. (48) by a diagonal matrix $\mathrm{diag}\left[\left(\tilde{M}g\right)^{-1}, \left(\tilde{M}g\right)^{-1}, \hat{E}\right]$, we transform Eq. (48) into the non-dimensional matrix equation

$$\begin{bmatrix} A_{11} & A_{12} & A_{13} \\ A_{21} & A_{22} & A_{23} \\ A_{31} & A_{32} & A_{33} \end{bmatrix} \begin{bmatrix} \tilde{u} \\ \tilde{U} \\ \tilde{i} \end{bmatrix} = \begin{bmatrix} 0 \\ 0 \\ 1 \end{bmatrix}, \tag{51}$$

where

$$\begin{aligned} &\tilde{u} = u/u_0, \quad \tilde{U} = U/u_0, \quad \tilde{i} = i/i_0, \\ &A_{11} = (1+\kappa_c) + 2\mathrm{j}(1+\varepsilon_c)\zeta_s\eta_s - (1+\mu_c)\eta_s^2, \\ &A_{12} = A_{21} = -(\kappa_c + 2\mathrm{j}\varepsilon_c\zeta_s\eta_s), \\ &A_{13} = -A_{23} = -\psi, \\ &A_{22} = (\kappa_m+\kappa_c) + 2\mathrm{j}(\varepsilon_m+\varepsilon_c)\zeta_s\eta_s - \mu_m\eta_s^2, \\ &A_{31} = (f_g-\kappa_g) + 2\mathrm{j}(f_g+\varepsilon_a-\varepsilon_g)\zeta_s\eta_s - (f_g-\mu_g)\eta_s^2, \\ &A_{32} = -2\mathrm{j}\varepsilon_a\zeta_s\eta_s, \\ &A_{33} = 1 + 2\mathrm{j}\varepsilon_e\zeta_s\eta_s. \end{aligned} \tag{52}$$

4.1. Stability

The characteristic equation of this example is derived from Eq. (38) or by equalling to zero the determinant of the coefficient matrix of Eq. (47) or (48) as given by

$$D = \begin{vmatrix} A_{11} & A_{12} & A_{13} \\ A_{21} & A_{22} & A_{23} \\ A_{31} & A_{32} & A_{33} \end{vmatrix} = \frac{1}{3!} e_{ijk} e_{lmn} A_{il} A_{jm} A_{kn} = 0, \tag{53}$$

where e_{ijk} denotes the permutation symbol [25]. By algebraic manipulation it is shown that the characteristic equation of the system is given by

$$D(\lambda) = a_5\lambda^5 + a_4\lambda^4 + a_3\lambda^3 + a_2\lambda^2 + a_1\lambda + a_0, \tag{54}$$

where

$$\lambda = \mathrm{j}\eta_s, \quad a_n = \frac{1}{n!}\frac{\mathrm{d}^n D}{\mathrm{d}\lambda^n}\bigg|_{\lambda=0}, \quad n = 0, 1, \ldots, 5. \tag{55}$$

Using the Hurwitz criteria [32], we obtain the necessary and sufficient conditions for stability as expressed by

$$a_5 > 0, \quad a_4 > 0, \quad \begin{vmatrix} a_4 & a_5 \\ a_2 & a_3 \end{vmatrix} > 0, \quad a_0 > 0,$$

$$\begin{vmatrix} a_4 & a_5 & 0 \\ a_2 & a_3 & a_4 \\ a_0 & a_1 & a_2 \end{vmatrix} > 0, \quad \begin{vmatrix} a_4 & a_5 & 0 & 0 \\ a_2 & a_3 & a_4 & 0 \\ a_0 & a_1 & a_2 & a_3 \\ 0 & 0 & a_0 & a_1 \end{vmatrix} > 0. \tag{56}$$

Eq. (53) is an algebraic equation of eigenvalue λ and all coefficients are real. Therefore, the complex solutions of this equation are conjugate. The necessary and sufficient conditions for stability require all eigenvalues to have negative real parts. To solve Eq. (53) or to determine the values of the Hurwitz's determinants in Eq. (56) requires a numerical method. For a large system, the numerical process is as follows:

(1) Determine all elements A_{ij} defined in Eq. (52) according to the chosen physical parameters as well as the value of λ.
(2) Calculate the constants a_i using Eqs. (54) and (55) through a loop summation process.
(3) Determine the stability of the system using Eq. (56).

4.2. Dynamic response and interactions

From Eq. (51), two equations similar to Eqs. (43) and (44) are derived in the form

$$\begin{aligned} &Z_{MD}\begin{bmatrix} \tilde{u} \\ \tilde{U} \end{bmatrix} = (Z_M + Z_{ME})\begin{bmatrix} \tilde{u} \\ \tilde{U} \end{bmatrix} = -A_{33}^{-1}\begin{bmatrix} A_{13} \\ A_{23} \end{bmatrix}, \\ &Z_M = \begin{bmatrix} A_{11} & A_{12} \\ A_{21} & A_{22} \end{bmatrix}, \quad Z_{ME} = -\begin{bmatrix} A_{13} \\ A_{23} \end{bmatrix} A_{33}^{-1}[\, A_{31} \quad A_{32}\,] \end{aligned} \tag{57}$$

and

$$\begin{aligned} &Z_{ED}\tilde{i} = (Z_E + Z_{EM})\tilde{i} = 1, \quad Z_E = A_{33}, \\ &Z_{EM} = -\begin{bmatrix} A_{31} & A_{32} \end{bmatrix}\begin{bmatrix} A_{11} & A_{12} \\ A_{21} & A_{22} \end{bmatrix}^{-1}\begin{bmatrix} A_{13} \\ A_{23} \end{bmatrix} = -\frac{A_{31}(A_{11} + 2A_{12} + A_{22})A_{13}}{A_{11}A_{22} - A_{12}A_{21}}. \end{aligned} \tag{58}$$

Eq. (57) can be further written as

$$\begin{aligned} &Z_{SD}\tilde{u} = F_S, \\ &Z_{SD} = (A_{11} - A_{13}A_{33}^{-1}A_{31}) - (A_{12} - A_{13}A_{33}^{-1}A_{32})(A_{22} - A_{23}A_{33}^{-1}A_{32})^{-1}(A_{21} - A_{23}A_{33}^{-1}A_{31}), \\ &F_S = -A_{13}A_{33}^{-1} + (A_{12} - A_{13}A_{33}^{-1}A_{32})(A_{22} - A_{23}A_{33}^{-1}A_{32})^{-1}A_{33}^{-1}A_{23}, \end{aligned} \tag{59}$$

allowing investigation of the impact of the excitation system on the characteristics of the structure.

Through these last three equations, the compatibility of the system and the interactions between the structure, exciter unit and the control systems are demonstrated. Here, Z_{MD} denotes the impedance of the mechanical system, including the structure and the mechanical parts of the exciter, influenced by the electrical and control system which adds an additional term Z_{ME} to the impedance Z_M of the pure mechanical system. Similarly, Z_{ED} denotes the impedance of the electrical and control system arising from the mechanical system which adds an additional term Z_{EM} to the dynamic impedance Z_E of the pure electrical and control system. Z_{SD} represents the impedance of the pure structure caused by the excitation system including the mechanical and electrical systems of the excitation system as well as the control system.

The non-dimensional responses (i.e. the displacement vector of the mechanical structure and the electric current of the electrical control unit) of the system subject to a unit input voltage can be solved from Eqs. (57) and (58). Here, we analyse the following special cases.

4.2.1. $\psi = 0 = \tilde{B}\hat{E}/R\tilde{M}g$

In this case, we have $A_{13} = A_{23} = 0$. Therefore, as indicated by Eqs. (57) and (58), the motions of both structure and magnetic body and the additional impedances Z_{ME} and Z_{EM} are all zero indicating no interaction between mechanical and electrical systems. Physically, $\psi = 0$ implies that there is no excitation force produced by the electric exciter to the structure.

4.2.2. $\varepsilon_a = 0 = \tilde{B}g/2\omega_s\zeta_s\hat{E}$

As shown in Eq. (50), the non-dimensional parameter ε_a involves the induced voltage of the exciter caused by the motion of its coil. Therefore, this case represents no induced voltage produced by the motion of the structure and the impedance of the electric system is not influenced by the structure's motion. If no active control is considered $A_{31} = 0$ then the additional impedance Z_{EM} is of zero value.

To demonstrate these cases, we choose the parameter values

$$\begin{aligned}&\text{Structure}: \tilde{M} = 1, \quad \tilde{K} = 1, \quad \zeta_s = 0.01.\\ &\text{Coil unit}: \mu_c = 0.05, \quad \kappa_c = 0.25, \quad \varepsilon_c = 2, \quad \varepsilon_e = 0.01.\\ &\text{Magnetic body unit}: \quad \mu_m = 0.4, \quad \kappa_m = 0.1, \quad \varepsilon_m = 2.\end{aligned} \tag{60}$$

These values give the frequency of the structure $\omega_s = 1$, the supporting frequency of the coil unit $\omega_c = 2.236$ and the suspension frequency of the magnetic body of the exciter $\omega_m = 0.5$. These values mirror a practical aircraft vibration test [15] where the first natural frequency of the aircraft is lower than the frequency of the coil support unit and the suspension frequency of the magnetic body is required to be lower than the first natural frequency of the aircraft.

Fig. 3 shows the dynamic responses of the interaction system subject to a unit input voltage. For example, as shown in Fig. 3(a) and (b), the motions of the structure and the exciter are zero when $\psi = 0$ and the electric current in the coil of the exciter vanishes when $\psi = 0$ or $\varepsilon_a = 0$.

4.3. Mechanical–electrical interactions with no active control

Let us assume that there are no active controls in the system, i.e. the control gains $g_s^{11} = 0$ ($s = u, v, a, f$), and therefore the parameters κ_g, ε_g, μ_g and f_g in Eq. (54) are all zero. The system described by Eq. (51) reduces to a mechanical structure–electromagnetic excitation interaction system in which $A_{31} = -A_{32}$ in Eqs. (57)–(59).

4.3.1. Mechanical impedance of the structure interacting with the excitation system

To investigate the impact of the excitation system on the natural characteristics of the structure, we use Eq. (52), to express Eq. (59) in the form

$$Z_{SD}^n = Z_s + \bar{z}_c + Z_{se} + Z_{sm}, \tag{61}$$

where superscript n of Z_{SD}^n denotes the case with no active control and

$$\begin{aligned}&Z_s = 1 + 2\mathrm{j}\zeta_s\eta_s - \eta_s^2, \quad Z_m = \kappa_m + 2\mathrm{j}\varepsilon_m\zeta_s\eta_s - \mu_m\eta_s^2, \quad Z_{sm} = -\frac{(z_c + Z_e)^2}{Z_m + z_c + Z_e},\\ &\bar{z}_c = \kappa_c + 2\mathrm{j}\varepsilon_c\zeta_s\eta_s - \mu_c\eta_s^2, \quad z_c = \kappa_c + 2\mathrm{j}\varepsilon_c\zeta_s\eta_s, \quad Z_{se} = \frac{2\mathrm{j}\varepsilon_a\psi\zeta_s\eta_s}{1 + 2\mathrm{j}\varepsilon_e\zeta_s\eta_s}.\end{aligned} \tag{62}$$

Here, Z_s represents the impedance of the structure with no interactions, $\bar{z}_c$ denotes the added impedance due to the pure mechanical impedance of the moving coil unit of the exciter but no electromagnetic interaction is involved which adds an additional impedance represented by Z_{se}, and Z_{sm} is the additional impedance caused by the motion of the magnetic body of the exciter. As shown in Eq. (62) for the impedance expressions, the real component involves the stiffness and mass characteristic and the imaginary component reflects the damping behaviour of the system.

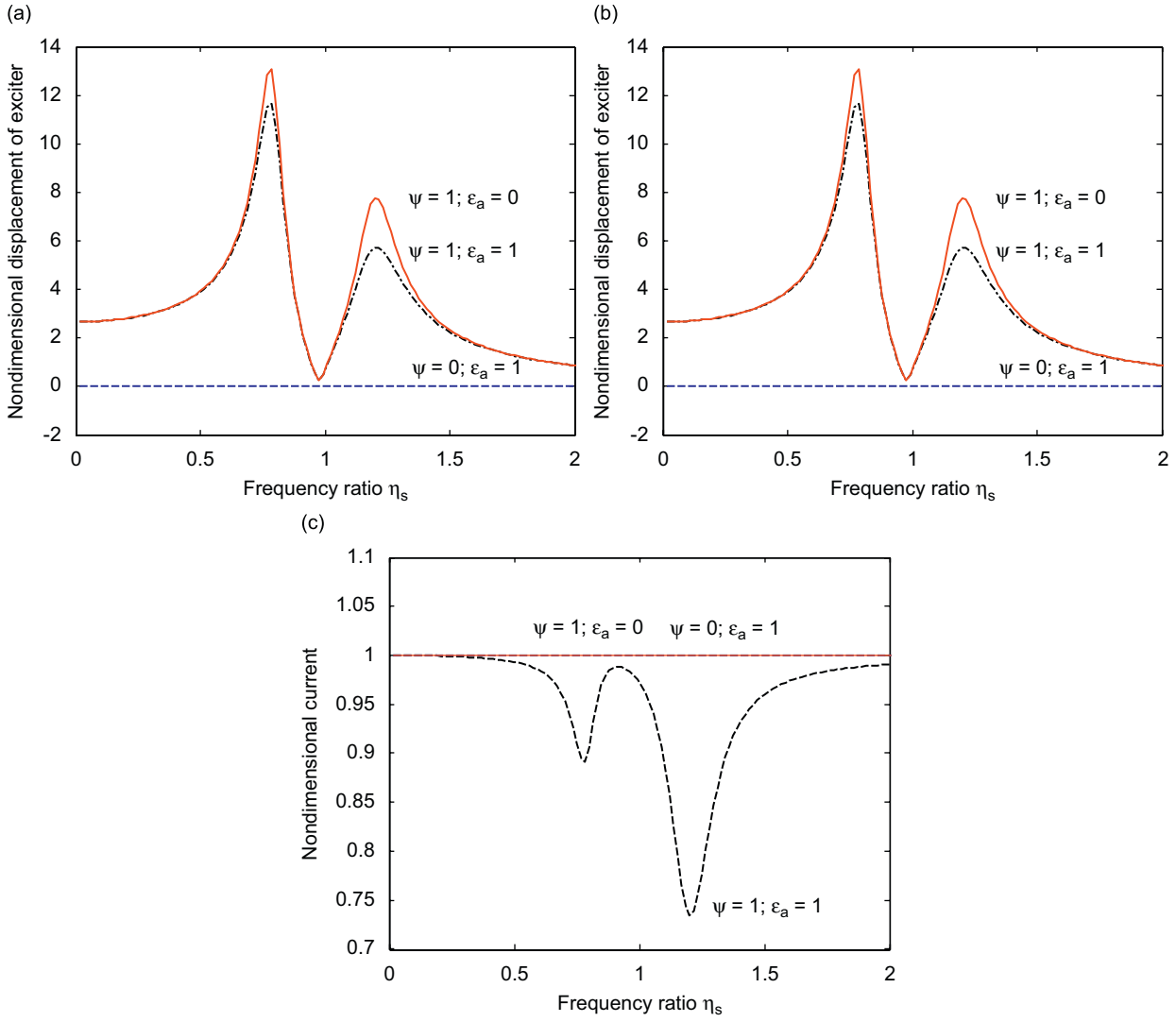

Fig. 3. Dynamic responses of the structure–electromagnetic excitation interaction system subject to a unit voltage: (a) non-dimensional displacement $\tilde{u}$ of the structure, (b) non-dimensional displacement $\tilde{U}$ of the exciter, and (c) non-dimensional current $\tilde{I}$ in the coil of the exciter.

The influence of the excitation system on the natural characteristics of the structure is summarised as follows:

(1) Due to the interaction between the structure and the suspension system of the magnetic body, the coupled system has two degrees of freedom as shown in Fig. 4. It is shown that only one peak exists in the receptance curve $\chi_s^n = 1/|Z_s|$ for the structure at its non-dimensional frequency $\eta_s = 1$ whereas two peaks occur in the receptance curve $\chi_{SD}^n = 1/|Z_{SD}^n|$ of the coupled system.

The effect of the magnetic body of the exciter on the structure is represented by the impedance Z_{sm}. If the magnetic body is fixed to a rigid foundation, its suspension stiffness $K = \infty$ and therefore $Z_{sm} = 0$ and the magnetic body does not influence the characteristic of the structure. As shown in Fig. 4, for a non-dimensional stiffness value $\kappa_m = 10$ of the suspension system of the magnetic body of the exciter one peak of the receptance curve $\chi_{SD}^n = 1/|Z_{SD}^n|$ of the coupled system disappears. For vibration tests in a range of lower excitation frequencies, to fix the magnetic body of the exciter on a solid foundation provides a good test design arrangement. However, for a vibration test involving higher frequencies, an idealised rigid foundation in a

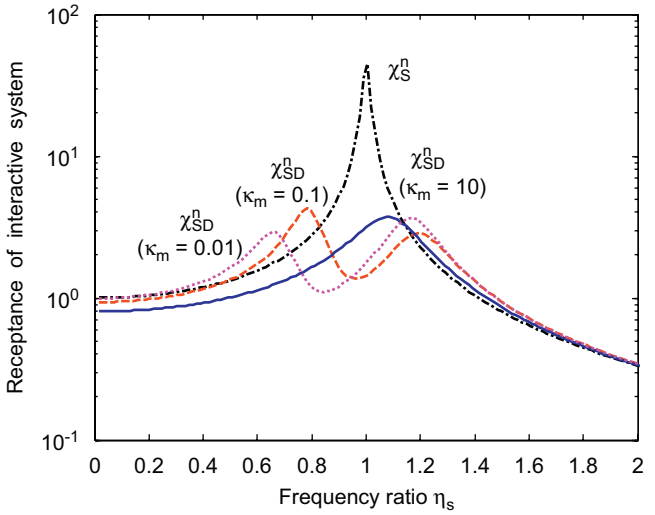

Fig. 4. The receptances of the interactive structure–excitation system influenced by the non-dimensional stiffness κ_m and compared to the receptance of the structure.

laboratory may not be realised. To solve this practical difficulty, the magnetic body of the exciter is supported by a very soft spring with a supporting frequency $\omega_m = \sqrt{K/M}$ at a value much lower than the first natural frequency ω_s of the structure, which can significantly reduce the effect of the suspension system of the exciter on the natural characteristics of the structure. As shown in Fig. 4, for a non-dimensional stiffness $\kappa_m = 0.01$ the right peak of the receptance curve $\chi^n_{SD} = 1/|Z^n_{SD}|$ of the coupled system is closer to the peak of the receptance curve for $\kappa_m = 10$. Therefore, the measured mechanical effect of the magnetic body of the exciter on the structure is largely reduced.

(2) The mechanical parts of the moving coil unit of the exciter add additional mass, damping and stiffness to the structure. Due to this effect, as shown in Fig. 4, there exist differences between the receptance curves of the structure and the coupled system idealised by a large non-dimensional stiffness $\kappa_m = 10$ of the suspension system of the magnetic body. To reduce the influence of the moving coil system on the natural characteristics of the structure, smaller values of mass m, stiffness k and damping c of the moving coil and its supporting elements are necessary. Fig. 5 shows the curves of the receptance of the coupled system impacted by the non-dimensional stiffness κ_c and mass μ_c of the moving coil unit of the exciter. It is found that a reduction of stiffness value κ_c moves the curve to the left and a reduction of mass value μ_c shifts the curve to the right. The case of $\kappa_c = 0$ gives a peak at a non-dimensional frequency less that 1 due to the effect of the mass of the coil system. Similarly, the case $\mu_c = 0$ produces a peak at a frequency larger than 1 due to the effect of the stiffness of the coil system. Naturally, as shown in Fig. 6, $\kappa_c = 0$ and $\mu_c = 0$ produce a peak at frequency $\eta_s = 1$ which is the same value as the natural frequency of the structure but the height of the peak is lower due to the damping of the coil system.

(3) As demonstrated in Eq. (62), the electromagnetic field interaction produces a complex impedance involving frequency-related damping and stiffness influences to the structure as given by

$$Z_{se} = \frac{2\mathrm{j}\varepsilon_a\psi\zeta_s\eta_s}{1+2\mathrm{j}\varepsilon_e\zeta_s\eta_s} = \frac{2\mathrm{j}\varepsilon_a\psi\zeta_s\eta_s + 4\varepsilon_a\varepsilon_e\psi\zeta_s^2\eta_s^2}{1+4\varepsilon_e^2\zeta_s^2\eta_s^2}, \tag{63}$$

in which the denominator is dependent on the non-dimensional excitation frequency η_s. Here two non-dimensional parameters ψ and ε_a are involved. To investigate the influence of the electromagnetic field on the natural characteristics of the structure, Fig. 7 shows the receptance $\chi^n_{SD} = 1/|Z^n_{SD}|$ of the coupled system with non-dimensional stiffness value $\kappa_m = 10$ dependent on values of ψ and ε_a. It is demonstrated that larger values of ψ or ε_a cause an increase in the damping characteristics of the system, which suggests that the additional impedance behaves mainly as a damping mechanism although its real part is non zero. Fig. 8 shows the case

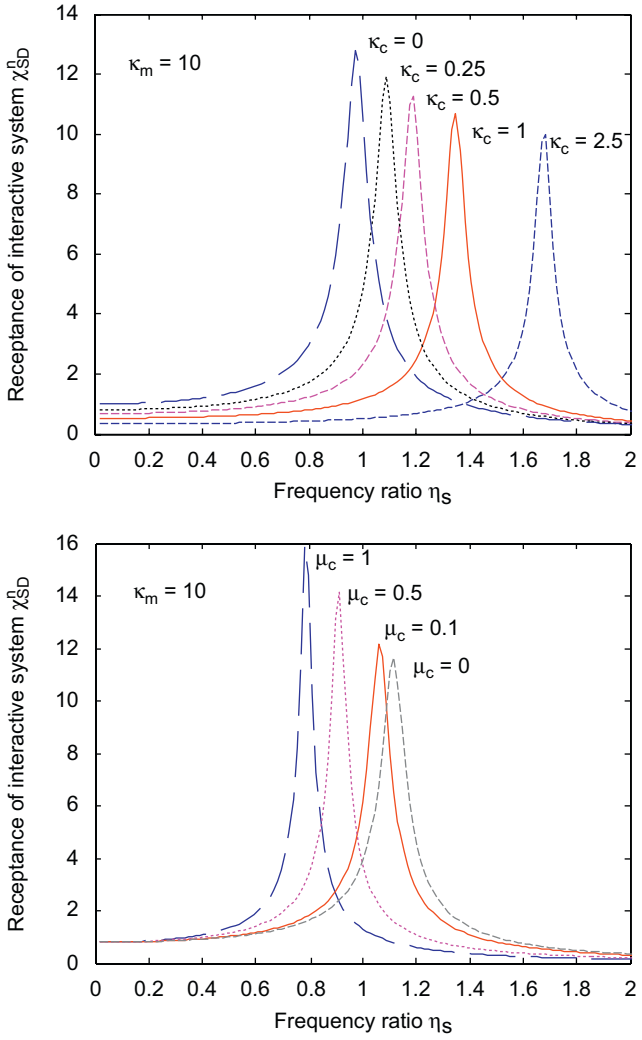

Fig. 5. The effect of the stiffness and mass of the moving coil system on the natural characteristics of the structure.

assuming $\kappa_m = 0.1$ and the results show the occurrence of two peaks with one introduced at the lower suspension frequency. It is also found that by increasing the value of ψ or ε_a increases the damping and decreases the value of the right peak associated with the structure's resonance. However, the value of the left peak associated with the suspension system increases, implying a large magnetic body motion in the vibration test which should be avoided. Therefore, for $\kappa_m = 0.1$ case, a good designed high quality exciter should posses a low value of ψ or ε_a.

4.3.2. Electrical impedance of the exciter influenced by mechanical motion

Eq. (58) provides description of the impedance Z^n_{ED} of the electrical excitation system influenced by the structure's motions which adds an additional impedance Z^n_{EM} to the electrical system. Here, superscript "n" represents the case of no active control in the system. A variation of frequency in the vibration test causes the denominator of Eq. (58) to reach a small value and therefore a large change of value of the added impedance Z^n_{EM}. For example, in the case of the magnetic body of the exciter fixed to a foundation, the stiffness of the suspension spring is infinite (i.e. $\kappa_m = \infty$) which reduces Eq. (58) to

$$Z^n_{ED} = Z_E + Z^n_{EM}, \quad Z^n_{EM} = \frac{2j\varepsilon_a\psi\zeta_s\eta_s}{(1+\kappa_c) + 2j(1+\varepsilon_c)\zeta_s\eta_s - (1+\mu_c)\eta_s^2}. \tag{64}$$

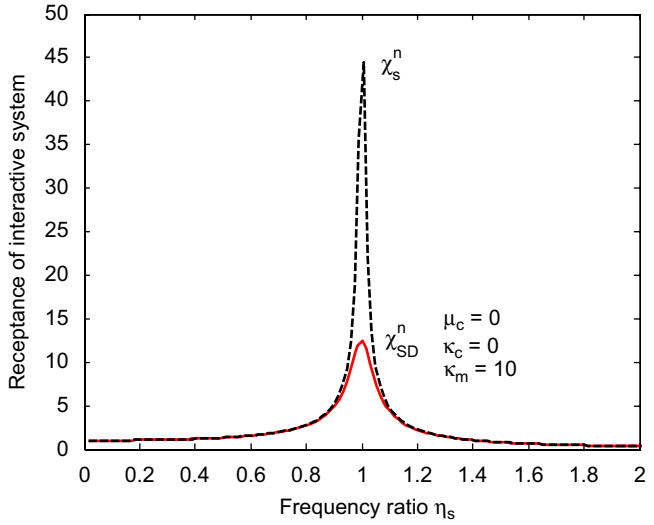

Fig. 6. The impact of the stiffness and mass of the coil system on the natural characteristics of the structure vanishes if $\kappa_c = 0$ and $\mu_c = 0$.

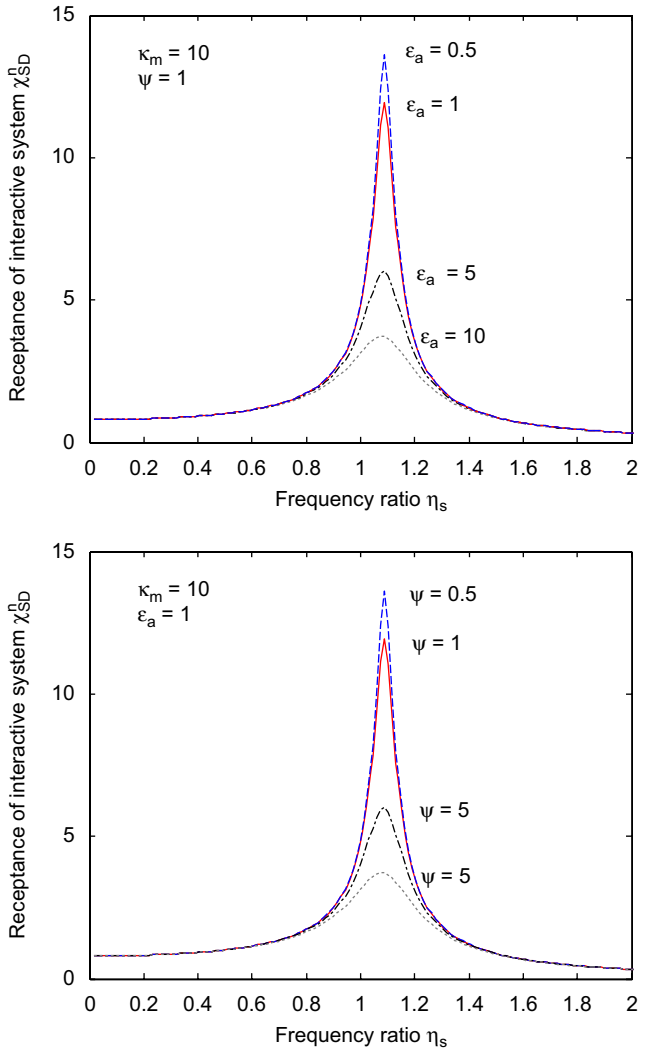

Fig. 7. The receptance of interactive system ($\kappa_m = 10$) effected by values of ψ and ε_a.

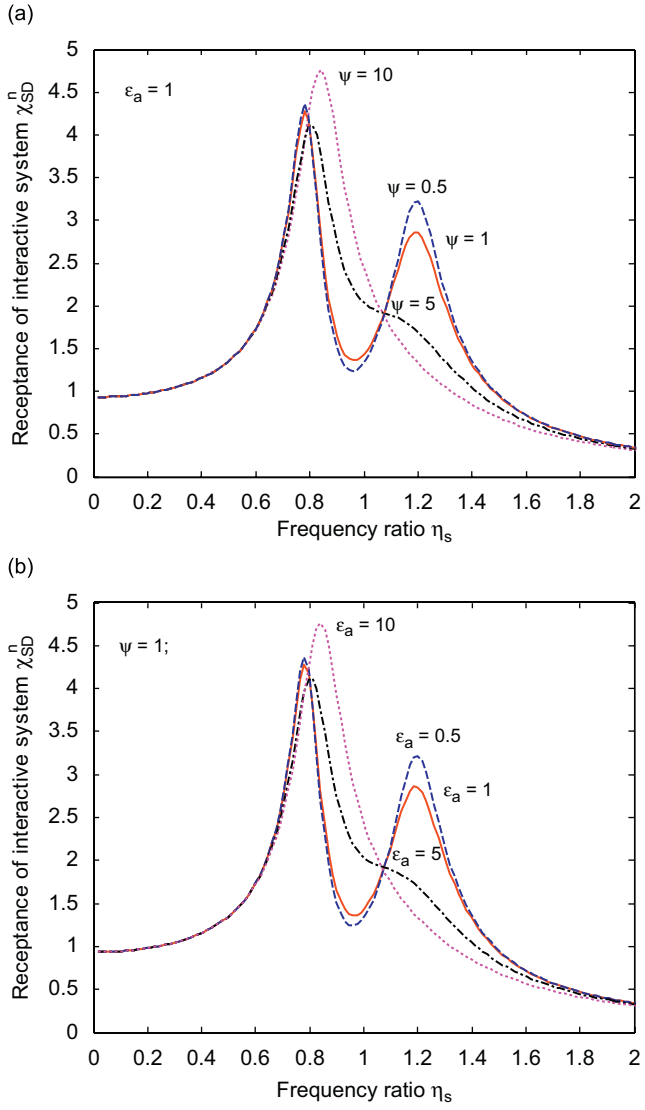

Fig. 8. The receptance of interactive system ($\kappa_m = 0.1$) influenced by values of ψ and ε_a.

For an excitation force frequency tending to the natural frequency value $\eta_s = \sqrt{(1+\kappa_c)/(1+\mu_c)}$ of the structure with the coil system, the added impedance

$$Z^n_{EM} = \frac{\varepsilon_a \psi}{1+\varepsilon_c} \tag{65}$$

can become a large value because of resonance.

Based on the assumed data given in Eq. (60), Fig. 9 illustrates the electrical receptance $\chi^n_E = 1/|Z_E|$ of the electric circuit and its dynamic receptance $\chi^n_{ED} = 1/|Z^n_{ED}|$ influenced by mechanical motions of the structure and the excitation system. It is shown that the electrical current supplying the moving coil is influenced by mechanical motions, especially in the range of frequency near to the vibration peaks. This is because the large added impedance caused by the mechanical motions changes the dynamic impedance of the electrical system. As a result, the large change of the output current $\tilde{i}$ and therefore the force applied to the structure are modified. In vibration tests it is therefore better to keep the amplitude of the excitation force unchanged with frequency, and the power amplifier system designed with a sufficiently large *negative current feedback* to suppress the current change caused by mechanical resonances.

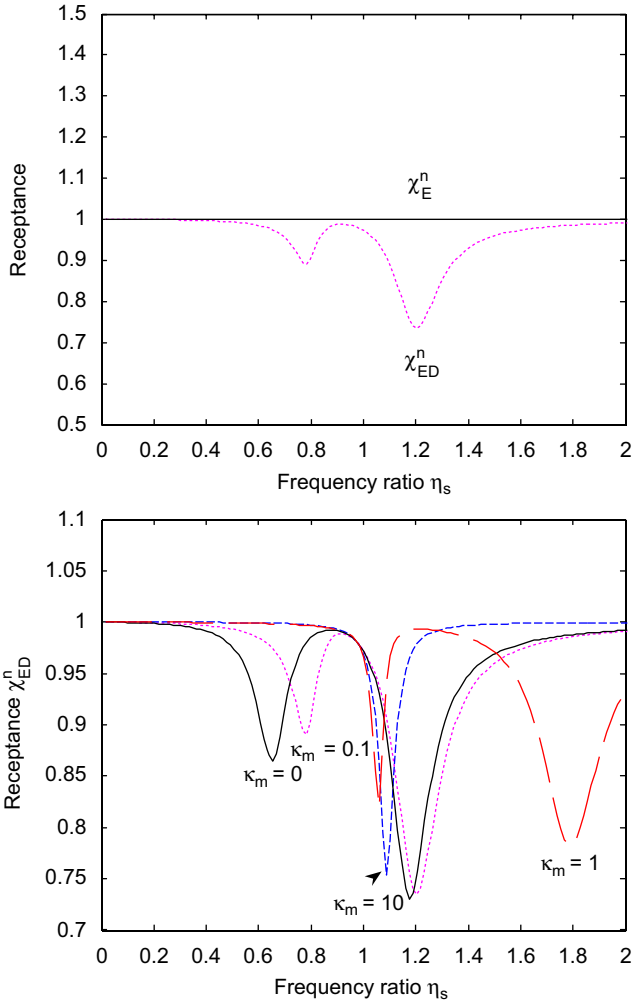

Fig. 9. The electrical receptance χ^n_E of the electrical circuit and its dynamic receptance χ^n_{ED} influenced by mechanical motions of the structure and the excitation system.

4.4. Control–structure interactions with active controls

We now discuss the CSIs arising in the coupled solution given by Eqs. (57)–(59). To compare findings with the no control case discussed in Section 4.3, the term A_{31} in Eq. (52) is rewritten as

$$A_{31} = -A_{32} + A^g_{31},$$
$$A^g_{31} = (f_g - \kappa_g) + 2\mathrm{j}(f_g - \varepsilon_g)\zeta_s\eta_s - (f_g - \mu_g)\eta_s^2, \tag{66}$$

where A^g_{31} represents the component associated with the control gain. The super- and subscript g denote control gain terms.

4.4.1. Mechanical impedance of the structure influenced by the control gains

From Eqs. (59) and (62), it follows that

$$Z^g_{SD} = Z_s + \bar{z}_c - A_{13}A_{33}^{-1}A_{31} - (A_{12} - A_{13}A_{33}^{-1}A_{32})(A_{22} - A_{23}A_{33}^{-1}A_{32})^{-1}(A_{21} - A_{23}A_{33}^{-1}A_{31}). \tag{67}$$

As shown in Eq. (66), a force feed-forward control influences not only the force applied to the structure but also the stiffness, damping and mass characteristics of the structure. A positive force-forward control gain increases the parameters of stiffness, damping and mass of the structure. Acceleration, velocity and

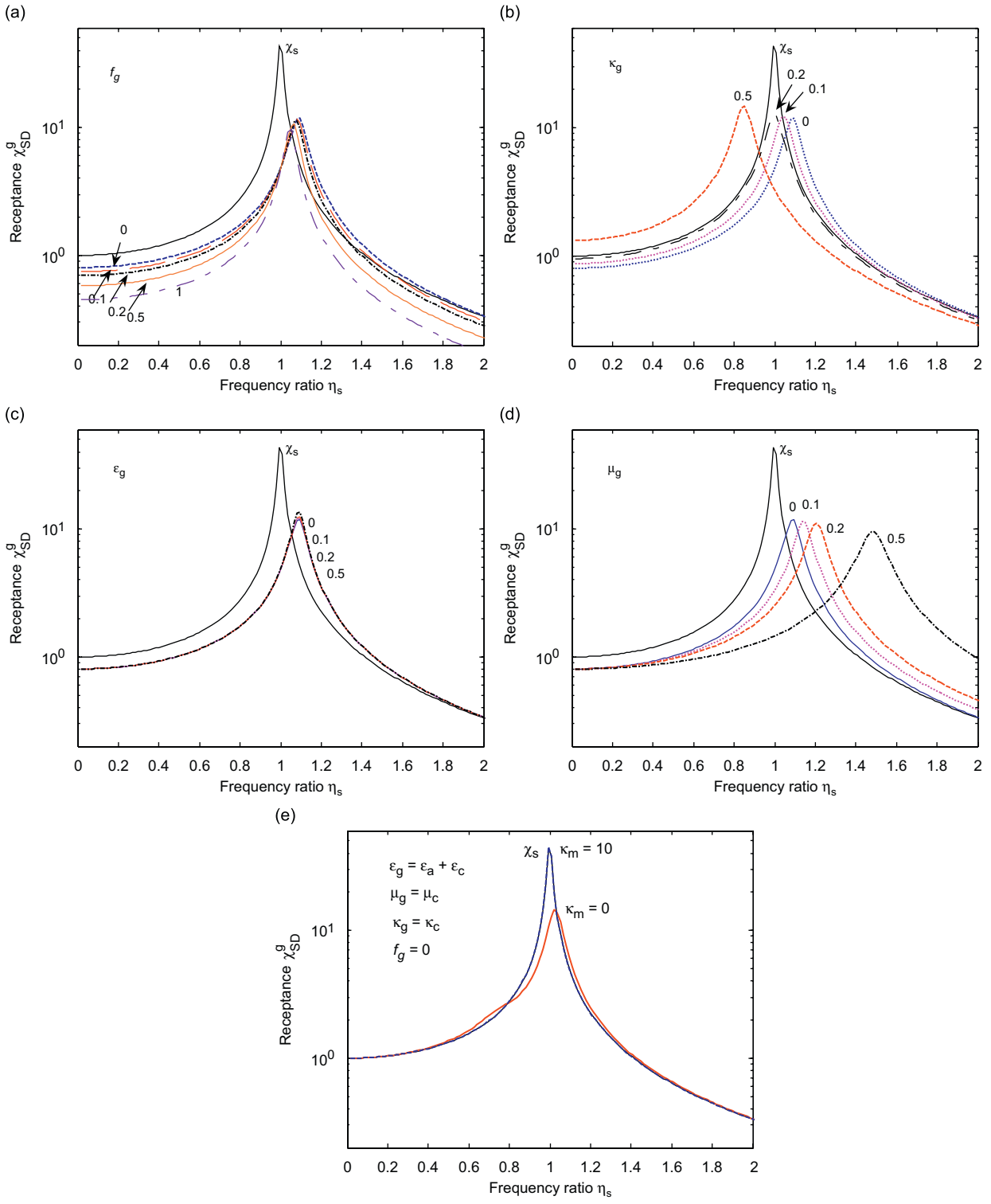

Fig. 10. The influence of active control on the receptance of the structure–control interaction system ($\kappa_m = 10$).

displacement feedback controls influence mass, damping and stiffness parameters of the structure, respectively. A positive motion (displacement, velocity or acceleration) feedback gain decreases the corresponding parameter of the structure. This mechanism suggests that active control can be used to reduce the influence of the mechanical components on the characteristics of the structure.

Fig. 10 shows the effect of active control on the receptance of the structure–control interaction system ($\kappa_m = 10$). It demonstrates that the force control parameter f_g adjusts the stiffness, damping and mass of the coupled system but does not shift the receptance curves along the frequency axis. Positive active stiffness (κ_g) and mass (μ_g) parameters shift the receptance curves to the left and right, respectively. The active damping parameter ε_g only changes the amplitude of the peaks of the receptance curves. By suitably choosing active control parameters, e.g. $f_g = 0$, $\kappa_g = \kappa_c$, $\mu_g = \mu_c$ and $\varepsilon_g = \varepsilon_a + \varepsilon_c$ we can reduce the added mass, stiffness and damping influences of the moving coil of the exciter on the receptance of the system. As illustrated in Fig. 10(e), by choosing suitable values of the active control parameters, the receptance of the coupled system ($\kappa_m = 10$) is exactly the same as the one for the structure.

4.4.2. *Electrical impedance of the control system affected by mechanical motion*

From Eq. (58), the dynamic impedance of the coupled system is rewritten as

$$Z^g_{ED} = Z_E + Z^g_{EM}, \quad Z^g_{EM} = -\frac{A_{31}(A_{11} + 2A_{12} + A_{22})A_{13}}{A_{11}A_{22} - A_{12}A_{21}}. \tag{68}$$

As shown in Eq. (66), active control can cause negative or positive influences on the impedance. Therefore, by suitably choosing the control gain value we may eliminate all effects of the motion on the electrical system. For example, in the case of the magnetic body fixed to a rigid foundation, Eq. (68) reduces to

$$Z^g_{EM} = \frac{\psi[(f_g - \kappa_g) + 2\mathrm{j}(f_g + \varepsilon_a - \varepsilon_g)\zeta_s\eta_s - (f_g - \mu_g)\eta_s^2]}{(1 + \kappa_c) + 2\mathrm{j}(1 + \varepsilon_c)\zeta_s\eta_s - (1 + \mu_c)\eta_s^2}. \tag{69}$$

By adjusting control parameters identified by subscript g, we can cause $Z^g_{EM} = 0$. Fig. 11 shows the effects of the control parameters on the dynamic electric receptance χ^g_{ED} of the structure–control interaction system adopting $\kappa_m = 10$. In comparison with the electrical receptance χ_E of the electric circuit it is not influenced by mechanical motions. In a similar manner as demonstrated in Fig. 10, the force control parameter f_g adjusts the stiffness, damping and mass of the coupled system and positive active stiffness (κ_g) and mass (μ_g) parameters move the receptance curves to the left and right, respectively. The active damping parameter ε_g only changes the amplitude of the peaks of the receptance curves. Also, by suitably choosing active control parameter values $f_g = \kappa_g = \mu_g$ and $\varepsilon_g = \varepsilon_a + f_g$ we can reduce the additional impedance Z^g_{ED} caused by the interaction, as demonstrated in Fig. 11(e). It is seen that by increasing the value of κ_m from 10 to 100, the magnetic body suspension spring tends to infinity and the effect of Z^g_{ED} on χ^g_{ED} gradually vanishes.

5. A vibration test

We now investigate the vibration test system shown in Fig. 12. The rigid bar of length L and mass density ρ per unit length is supported by two springs of stiffness $\tilde{K}$ and two dampers of damping coefficient $\tilde{C}$. The bar is vibrated by two electromagnetic exciters and, for simplicity, the supporting magnetic bodies and electric channels, etc., as shown in Figs. 1 and 2 for the complete generalised model, have been omitted. The aim of the vibration test is to measure the two natural frequencies of the system. Due to the effect of the stiffness (k), damping (c) and mass (m) of the coil system of each exciter, the measured frequencies are not the real frequencies of the system investigated. Active feedback controls are introduced to eliminate the effects of the excitation system in order to obtain the actual frequencies of the system.

The equations describing the natural vibration of this system are expressed in the matrix form

$$\begin{bmatrix} \rho L/3 & \rho L/6 \\ \rho L/6 & \rho L/3 \end{bmatrix} \begin{Bmatrix} \ddot{u}_1 \\ \ddot{u}_2 \end{Bmatrix} + \begin{bmatrix} \tilde{C} & 0 \\ 0 & \tilde{C} \end{bmatrix} \begin{Bmatrix} \dot{u}_1 \\ \dot{u}_2 \end{Bmatrix} + \begin{bmatrix} \tilde{K} & 0 \\ 0 & \tilde{K} \end{bmatrix} \begin{Bmatrix} u_1 \\ u_2 \end{Bmatrix} = \begin{Bmatrix} 0 \\ 0 \end{Bmatrix}. \tag{70}$$

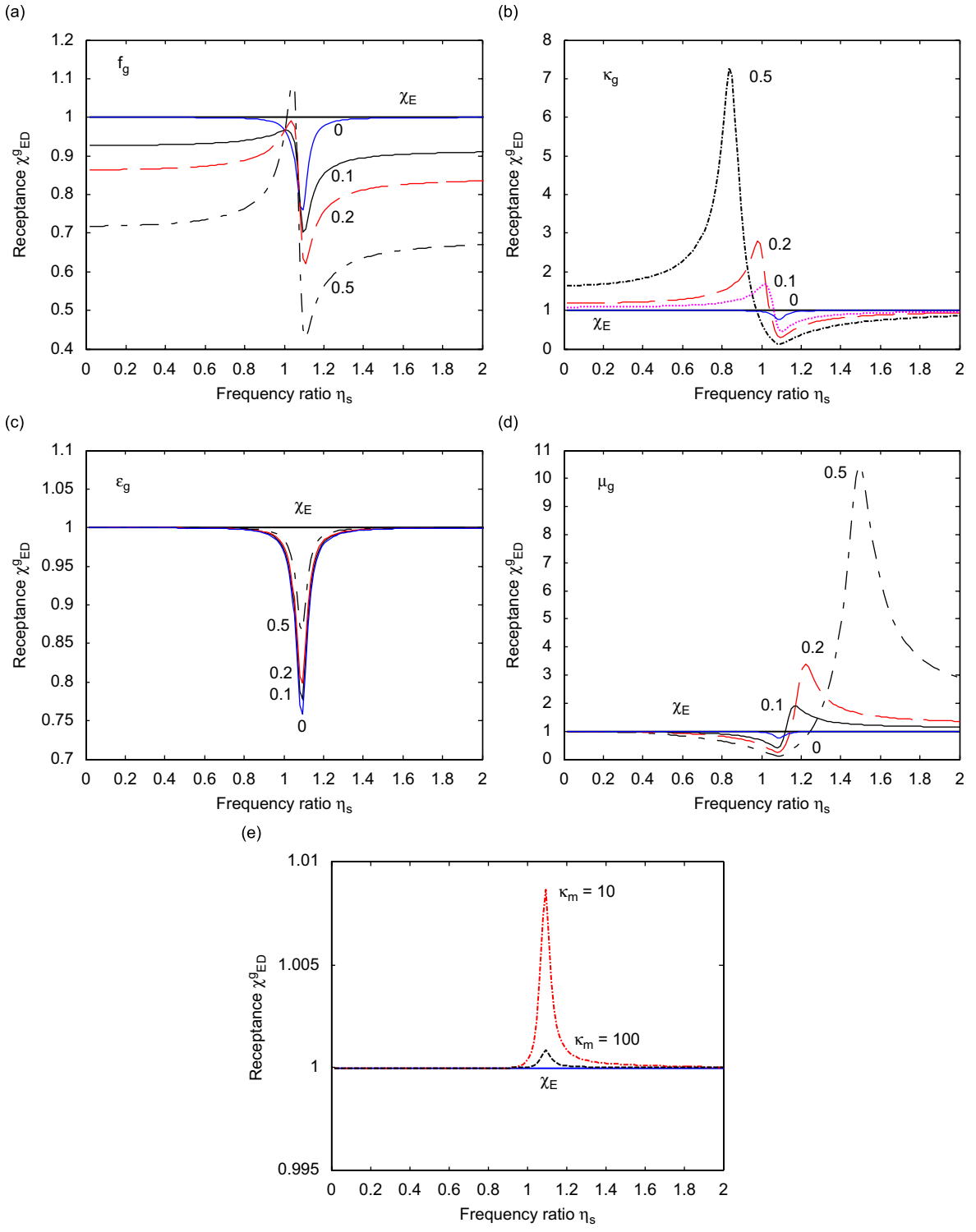

Fig. 11. The influence of the control parameters on the dynamic electric receptance χ^g_{ED} of the structure–control interaction system with $\kappa_m = 10$ compared to the electrical receptance χ_E of the electrical circuit not influenced by mechanical motions. In (c), the active control parameters $f_g = \kappa_g = \mu_g$ and $\varepsilon_g = \varepsilon_a + f_g$ are chosen to reduce the influence of the additional impedance Z^g_{ED} caused by the interaction.

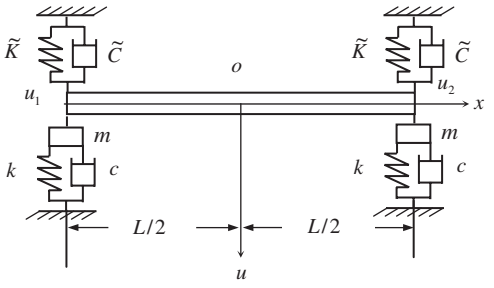

Fig. 12. A rigid bar supported by two support units and excited by two electromagnetic exciters to measure the system's natural frequencies. The two electromagnetic exciters also play the role of two active control actuators for which the electric energy supply channels are omitted.

The natural frequencies and mode shapes of the system are

$$\omega_{s1}=\sqrt{\frac{2\tilde{K}}{\rho L}},\quad \omega_{s2}=\sqrt{\frac{6\tilde{K}}{\rho L}},\quad \tilde{\mathbf{\Phi}}=[\,\varphi^1\quad\varphi^2\,]=\begin{bmatrix}1 & 1\\ 1 & -1\end{bmatrix}. \tag{71}$$

Therefore, the matrices $\tilde{\mathbf{M}}$, $\tilde{\mathbf{K}}$, $\tilde{\mathbf{C}}$ in Eq. (39) now take the following forms:

$$\tilde{\mathbf{M}}=\begin{bmatrix}1 & 1\\ 1 & -1\end{bmatrix}\begin{bmatrix}\rho L/3 & \rho L/6\\ \rho L/6 & \rho L/3\end{bmatrix}\begin{bmatrix}1 & 1\\ 1 & -1\end{bmatrix}=\tilde{M}\boldsymbol{\mu}_s,\quad \tilde{M}=\rho L,\quad \boldsymbol{\mu}_s=\begin{bmatrix}1 & \\ & 1/3\end{bmatrix}, \tag{72}$$

$$\tilde{\mathbf{K}}=\begin{bmatrix}1 & 1\\ 1 & -1\end{bmatrix}\begin{bmatrix}\tilde{K} & 0\\ 0 & \tilde{K}\end{bmatrix}\begin{bmatrix}1 & 1\\ 1 & -1\end{bmatrix}=\tilde{K}\boldsymbol{\kappa}_s,\quad \boldsymbol{\kappa}_s=2\hat{\mathbf{I}}, \tag{73}$$

$$\tilde{\mathbf{C}}=\begin{bmatrix}1 & 1\\ 1 & -1\end{bmatrix}\begin{bmatrix}\tilde{C} & 0\\ 0 & \tilde{C}\end{bmatrix}\begin{bmatrix}1 & 1\\ 1 & -1\end{bmatrix}=\tilde{C}\boldsymbol{\varepsilon}_s,\quad \boldsymbol{\varepsilon}_s=2\hat{\mathbf{I}}. \tag{74}$$

We assume that the two exciters have the same mechanical characteristics and their power supply units have the same perfect direct current characteristics. As a result of these assumptions we have

$$\begin{aligned}&\mathbf{H}_b=\begin{bmatrix}g_b^{11} & g_b^{12}\\ g_b^{21} & g_b^{22}\end{bmatrix}\quad (b=a,v,u,f),\quad \mathbf{H}=\begin{bmatrix}1 & \\ & 1\end{bmatrix}=\hat{\mathbf{I}},\ \text{and}\ \tilde{\mathbf{B}}=\tilde{B}\hat{\mathbf{I}},\\ &\mathbf{R}=R\hat{\mathbf{I}},\quad \mathbf{L}=L\hat{\mathbf{I}},\quad \hat{\mathbf{E}}=\hat{E}[\,1\quad 1\,]^{\mathrm{T}}.\end{aligned} \tag{75}$$

To obtain non-dimensional equations, we use the standard displacement u_0 and electric current i_0, as given in Eq. (49), i.e. $u_0=\tilde{M}g/\tilde{K}$, $i_0=\hat{E}/R$ from which we introduce the following non-dimensional parameters, vectors and matrices:

$$\begin{aligned}&\eta_s=\Omega/\omega_s,\quad \omega_s=\sqrt{\tilde{K}/\tilde{M}},\quad \zeta_s=\frac{\tilde{C}}{2\tilde{M}\omega_s},\\ &\boldsymbol{\psi}=\frac{\tilde{B}\hat{E}}{R\tilde{M}g}\hat{\mathbf{I}}=\frac{\tilde{B}i_0}{\tilde{M}g}\hat{\mathbf{I}},\quad \zeta_s\boldsymbol{\varepsilon}_a=\frac{\tilde{B}g}{2\omega_s\hat{E}}\hat{\mathbf{I}}=\frac{\tilde{B}g\omega_s^{-1}}{2\hat{E}}\hat{\mathbf{I}},\quad \zeta_s\boldsymbol{\varepsilon}_e=\frac{L\omega_s}{2R}\hat{\mathbf{I}},\\ &\boldsymbol{\kappa}_c=(k/\tilde{K})\hat{\mathbf{I}},\quad \boldsymbol{\varepsilon}_c=(c/\tilde{C})\hat{\mathbf{I}},\quad \boldsymbol{\mu}_c=(m/\tilde{M})\hat{\mathbf{I}},\\ &\boldsymbol{\kappa}_m=(K/\tilde{K})\hat{\mathbf{I}},\quad \boldsymbol{\varepsilon}_m=(C/\tilde{C})\hat{\mathbf{I}},\quad \boldsymbol{\mu}_m=(M/\tilde{M})\hat{\mathbf{I}},\\ &\boldsymbol{\kappa}_g=\frac{\tilde{M}g}{\tilde{K}\hat{E}}\begin{bmatrix}g_u^{11} & g_u^{12}\\ g_u^{21} & g_u^{22}\end{bmatrix},\quad \boldsymbol{\varepsilon}_g=\frac{\tilde{M}g}{\tilde{C}\hat{E}}\begin{bmatrix}g_v^{11} & g_v^{12}\\ g_v^{21} & g_v^{22}\end{bmatrix},\quad \boldsymbol{\mu}_g=\frac{g}{\hat{E}}\begin{bmatrix}g_a^{11} & g_a^{12}\\ g_a^{21} & g_a^{22}\end{bmatrix},\quad \mathbf{f}_g=\frac{\tilde{M}g}{\hat{E}}\begin{bmatrix}g_f^{11} & g_f^{12}\\ g_f^{21} & g_f^{22}\end{bmatrix},\\ &\tilde{\mathbf{Q}}=\mathbf{Q}/u_0,\quad \tilde{\mathbf{U}}=\mathbf{U}/u_0,\quad \tilde{\mathbf{I}}=\mathbf{I}/i_0.\end{aligned} \tag{76}$$

By applying these non-dimensional variables and matrices, we now transform Eq. (42) into the following form:

$$\begin{bmatrix} \mathbf{A}_{11} & \mathbf{A}_{12} & \mathbf{A}_{13} \\ \mathbf{A}_{21} & \mathbf{A}_{22} & \mathbf{A}_{23} \\ \mathbf{A}_{31} & \mathbf{A}_{32} & \mathbf{A}_{33} \end{bmatrix} \begin{bmatrix} \tilde{\mathbf{Q}} \\ \tilde{\mathbf{U}} \\ \tilde{\mathbf{I}} \end{bmatrix} = \begin{bmatrix} \mathbf{0} \\ \mathbf{0} \\ \mathbf{1} \end{bmatrix}, \quad \mathbf{0} = \begin{bmatrix} 0 \\ 0 \end{bmatrix}, \quad \mathbf{1} = \begin{bmatrix} 1 \\ 1 \end{bmatrix}, \tag{77}$$

where

$$\begin{aligned} \mathbf{A}_{11} &= (\boldsymbol{\kappa}_s + 2\mathrm{j}\boldsymbol{\varepsilon}_s\zeta_s\eta_s - \boldsymbol{\mu}_s\eta_s^2) + \tilde{\boldsymbol{\Phi}}^{\mathrm{T}}(\boldsymbol{\kappa}_c + 2\mathrm{j}\boldsymbol{\varepsilon}_c\zeta_s\eta_s - \boldsymbol{\mu}_c\eta_s^2)\tilde{\boldsymbol{\Phi}}, \\ \mathbf{A}_{12} &= \mathbf{A}_{21}^{\mathrm{T}} = -\tilde{\boldsymbol{\Phi}}^{\mathrm{T}}(\boldsymbol{\kappa}_c + 2\mathrm{j}\boldsymbol{\varepsilon}_c\zeta_s\eta_s), \\ \mathbf{A}_{13} &= -\tilde{\boldsymbol{\Phi}}^{\mathrm{T}}\boldsymbol{\psi}, \\ \mathbf{A}_{23} &= \boldsymbol{\psi}, \\ \mathbf{A}_{22} &= (\boldsymbol{\kappa}_m + \boldsymbol{\kappa}_c) + 2\mathrm{j}(\boldsymbol{\varepsilon}_m + \boldsymbol{\varepsilon}_c)\zeta_s\eta_s - \boldsymbol{\mu}_m\eta_s^2, \\ \mathbf{A}_{31} &= [-\boldsymbol{\kappa}_g + 2\mathrm{j}(\boldsymbol{\varepsilon}_a - \boldsymbol{\varepsilon}_g)\zeta_s\eta_s + (\mathbf{f}_g\boldsymbol{\mu}_c + \boldsymbol{\mu}_g)\eta_s^2]\tilde{\boldsymbol{\Phi}}, \\ \mathbf{A}_{32} &= -\mathbf{f}_g(\boldsymbol{\kappa}_m + 2\mathrm{j}\boldsymbol{\varepsilon}_m\zeta_s\eta_s - \boldsymbol{\mu}_m\eta_s^2) - 2\mathrm{j}\boldsymbol{\varepsilon}_a\zeta_s\eta_s, \\ \mathbf{A}_{33} &= \hat{\mathbf{I}} + 2\mathrm{j}\boldsymbol{\varepsilon}_e\zeta_s\eta_s. \end{aligned} \tag{78}$$

Eq. (43) and the corresponding displacement impedance matrices are given by

$$\begin{aligned} &(\mathbf{Z}_M + \mathbf{Z}_{ME}) \begin{bmatrix} \tilde{\mathbf{Q}} \\ \tilde{\mathbf{U}} \end{bmatrix} = -\begin{bmatrix} \mathbf{A}_{13} \\ \mathbf{A}_{23} \end{bmatrix} \mathbf{Z}^{-1}\mathbf{1}, \\ &\mathbf{Z}_M = \begin{bmatrix} \mathbf{A}_{11} & \mathbf{A}_{12} \\ \mathbf{A}_{21} & \mathbf{A}_{22} \end{bmatrix}, \\ &\mathbf{Z}_{ME} = \begin{bmatrix} -\mathbf{A}_{13}\mathbf{A}_{33}^{-1}\mathbf{A}_{31} & -\mathbf{A}_{13}\mathbf{A}_{33}^{-1}\mathbf{A}_{32} \\ -\mathbf{A}_{23}\mathbf{A}_{33}^{-1}\mathbf{A}_{31} & -\mathbf{A}_{23}\mathbf{A}_{33}^{-1}\mathbf{A}_{32} \end{bmatrix}. \end{aligned} \tag{79}$$

For numerical calculations, we assume that the magnetic bodies of the two exciters are fixed to a rigid foundation and that their chosen parameter values are given by $\boldsymbol{\psi} = \hat{\mathbf{I}} = \boldsymbol{\varepsilon}_a$ and $\boldsymbol{\varepsilon}_e = \mathbf{0}$. Here, $\boldsymbol{\varepsilon}_e = \mathbf{0}$ implies that the electrical induction of the moving coil is neglected. Fig. 13 shows the receptance curves of the system,

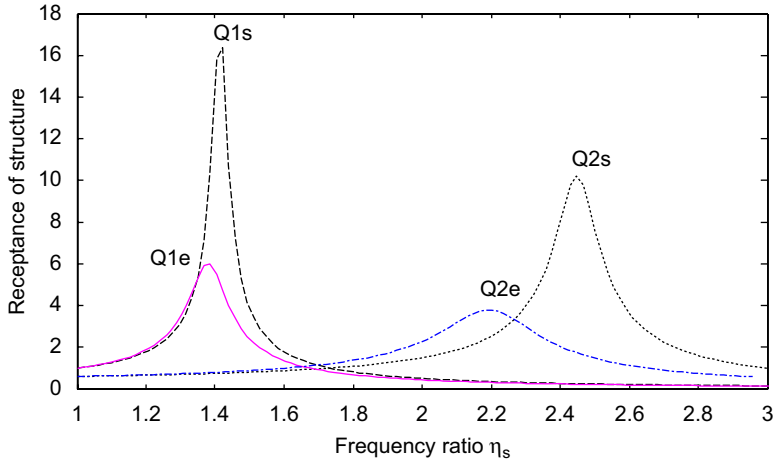

Fig. 13. The impact of exciters (see Fig. 12) on the receptance of the structure (structure not influenced Q1s and Q2s; influenced Q1e and Q2e).

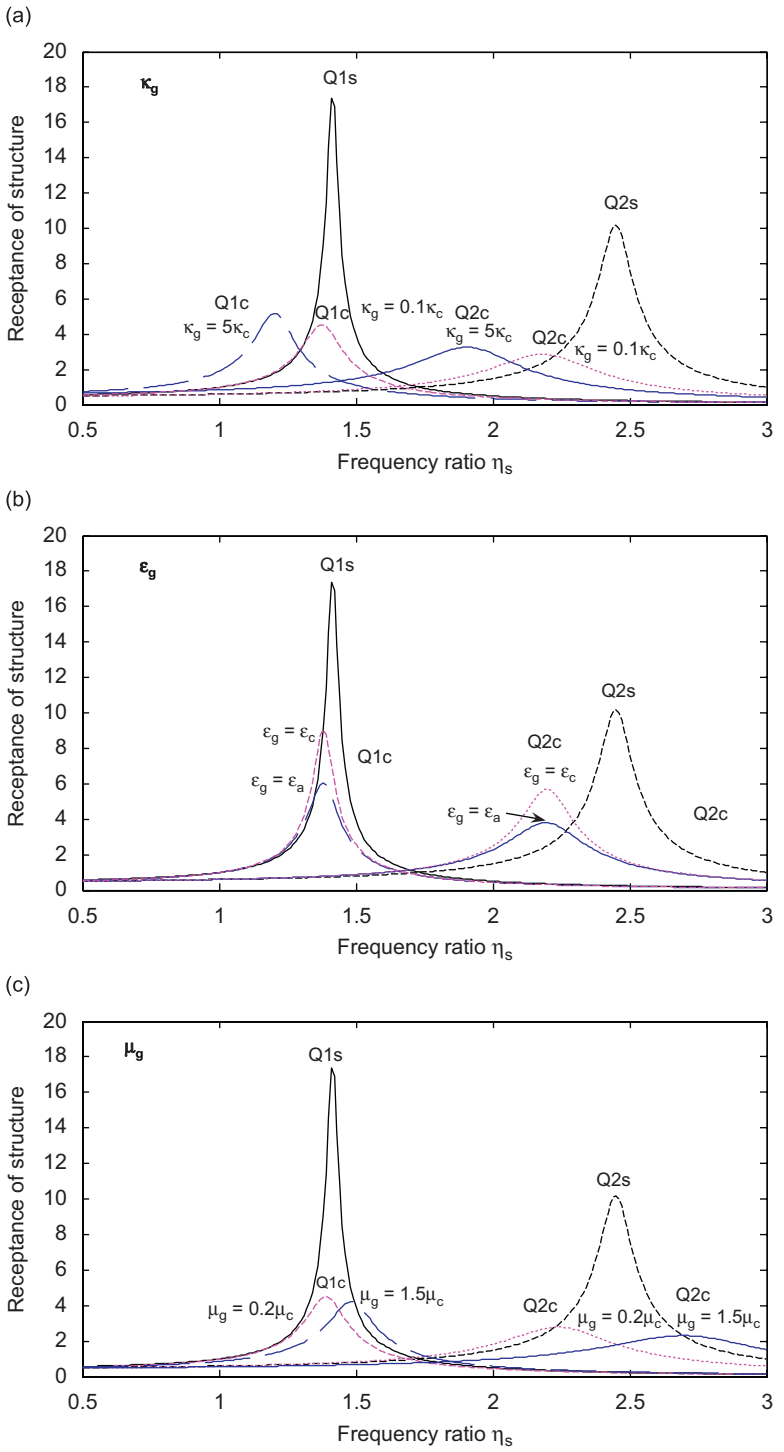

Fig. 14. The receptances of the structure influenced by (a) displacement, (b) velocity and (c) acceleration feedback controls (structure Q1s and Q2s; controlled Q1c and Q2c).

where Q1s and Q2s represent the two peaks of the structure not influenced by the exciters and Q1e and Q2e denote the results caused by the two exciters. Due to the influence of the two exciters, the original peaks move to the left, so that the measured natural frequencies of the structure influenced by the exciters are lower than

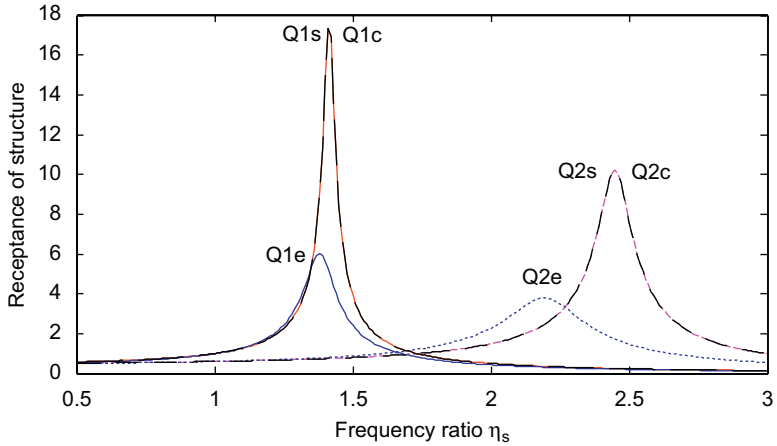

Fig. 15. An illustration of the total elimination of the influence of exciters by choosing suitable displacement, velocity and acceleration feedback controls described by Eq. (50). Here, Q1s and Q2s denotes the receptance of the structure with no contribution from exciters, Q1e and Q2e denote influence of exciters, and Q1c and Q2c represent the results obtained using feedback control to eliminate the influence of exciters.

the real ones. Fig. 14(a)–(c) provides predictions derived using an active feedback control with inputs of displacement ($\boldsymbol{\kappa}_g$), velocity ($\boldsymbol{\varepsilon}_g$) and acceleration ($\boldsymbol{\mu}_g$), which adjust the stiffness, damping and inertial (mass) parameters, respectively, as discussed in Section 4. Fig. 15 illustrates results for an active feedback control satisfying

$$\boldsymbol{\kappa}_g = \boldsymbol{\kappa}_c, \quad \boldsymbol{\varepsilon}_g = \boldsymbol{\varepsilon}_c + \boldsymbol{\varepsilon}_a, \quad \boldsymbol{\mu}_g = \boldsymbol{\mu}_c. \tag{80}$$

It is seen that the influence of the exciters on the structure are totally eliminated and therefore the receptance is exactly the same as the one for the original structure allowing the two natural frequencies of the system to be determined accurately. It is noted that the full compensation condition given in Eq. (80) only involves the parameters of the exciter which should be known for any well-designed exciter. Therefore, a full compensated exciter can be designed using active control techniques. Some of these techniques, such as, an electrically generated stiffness (displacement feedback) and damper (velocity feedback) have been successfully employed in aircraft vibration tests [15].

6. Conclusions and discussions

A generalised mathematical model and corresponding analysis method for integrated multi-channel vibration structure–control interaction systems are developed. The theory includes the following aspects:

(1) the governing equations describe a generalised interdisciplinary interaction system consisting of an elastic structure, multi-channel electromagnetic excitation and control units;
(2) the generalised mathematical model presented allows analysis of the stability and mechanical and electrical dynamic responses of the system;
(3) the influence of the electrical system or active control unit on the dynamic characteristics of the mechanical system and vice versa can be analysed using the developed generalised mathematical model,
(4) the number of degrees of freedom admitted to describe the structure is arbitrary, which can be chosen depending on the complexity of the problem under investigation;
(5) the theoretical number of possible control channels is arbitrary, with its value chosen depending on the requirements of the problem;
(6) motion feedback control including displacements, velocities and accelerations at multi-points on the structure and multi-force feed-forward control strategies are considered and their influences adjusted by the four control gain parameters in the mathematical model;

(7) mechanical–electrical interaction systems with no active control are special cases of the generalised system in which all active control gains are set to zero.

The underlying mechanisms of mechanical system (including structure and exciter)–electrical control system interactions are described and investigated by introducing an additional impedance matrix of the control system to the mechanical system and vice versa. The generalised theory provides a basis to investigate the following engineering problems: (1) to measure exactly the dynamic parameters of the structure using active control to reduce the influences of mechanical parts and electrical factors of the exciter and control systems; (2) to design a more effective and accurate control system to include the influences of mechanical motions; (3) to design a high quality excitation system for use in vibration tests.

Based on the developed general formulations, a single one-channel system and a more complex system are investigated using non-dimensional parameters to demonstrate the applicability of the general theory and analysis methods.

For practical applications of the developed mathematical model and solution approaches, the following points need consideration:

(1) The model is based on a linear approximation which assumes the structure, actuators and control units are governed by linear equations and the control power may be infinite. In practice, a mechanical or electrical system is nonlinear and the power is finite. For a system with very significant nonlinear elements, an accurate nonlinear model is required. The limits of control power, geometrical space to fix related equipment of the active control system, etc., require additional consideration.
(2) To design an effective vibration control system, many analytical, numerical and experimental tasks need addressing. This study provides an integrated mathematical model as well as numerical approach to consider all interaction mechanisms for structure–control interaction systems, which, in the design process, can be adopted to determine the necessary parameters by numerical calculations. For a real design, due to the approximations in the mathematical model, experimental information is necessary to check, to modify and to improve the initial design. This investigation presents a fundamental basis on which to address some gaps arising in the analysis of structure–control interactions. The mathematical model has partially been confirmed successfully by practical experiments [15] and in combination with known issues involved in designing suitable systems [22], practical problems may be better addressed.
(3) The developed mathematical model uses the orthogonal modes and frequencies of natural vibrations of the involved structures. As used in aircraft designs and vibration analysis, these data on the natural vibrations of structures are obtained using two approaches. In the design stage, when the aircraft has not been produced, a full aircraft structural finite element analysis in association with computer-aided design has to be carried out to obtain these data for other dynamic analysis, such as flutter analysis and control system design. Naturally, these data in the design stage can be modified to satisfy various requirements. While the first two prototypes of the designed airplane are produced, the first one with only structure elements is used for its static breakdown test to confirm its designed strength and the second one with other equipments is used for its ground vibration test and then flight test. In the ground vibration test of full scale aircraft [15], the natural orthogonal modes and frequencies of the aircraft are measured. These measured data are used for the further flutter analysis of aircraft, which is the most important task to confirm its dynamical safety before a flight test. Due to this reason, the measured data are expected to be accurate with as less as possible affects by the test equipments. Therefore, applications of feedback controls to eliminate vibrators affects on aircraft test are required [15].
(4) The governing equations in time domain given in Section 2 of this paper are generalised ones which do not require the transfer functions of control systems being constant, although it is normally designed having very good constant frequency characteristics in lower frequency range for aircraft sinusoidal vibration test system. However, if disturbance excitations are not in sinusoidal forms, the equations in frequency domain based on a sinusoidal force, given in Section 3, can not be directly used. There are two following ways to carry out the analysis for this case. The first one is to complete a frequency analysis to obtain all harmonic components of the given disturbance and then the superposition principle is used through a summation of the results of all harmonic excitation components to obtain the integrated result. The second one is a more

generalised approach that requires a frequency transformation of the equations in Section 2 to obtain the equations in frequency domain in which the frequency spectrum of arbitrary prescribed excitations, such as a mechanical impulse, is involved. As suggested by referees, this is a further investigation regarding to practical applications of the method to more complex practical cases.

Appendix A

On using the mode transformation in Eq. (23) in association with orthogonality relationships, i.e. Eqs. (20) and (21), we find that Eq. (15) describing the dynamics behaviour of the structure is transformed into

$$\tilde{\mathbf{M}}\,\ddot{\mathbf{q}} + (1+\mathrm{j}\zeta)\tilde{\mathbf{K}}\,\mathbf{q} = -\tilde{\mathbf{\Phi}}^{\mathrm{T}}\tilde{\mathbf{f}} = \bar{\mathbf{F}}, \tag{A.1}$$

where $\bar{\mathbf{F}}$ represents a generalised force vector in the mode coordinate system. The equation describing the motion of the Jth mode is written as

$$\tilde{M}^J\ddot{q}^J + (1+\mathrm{j}\zeta)\tilde{K}^J q^J = \bar{F}^J. \tag{A.2}$$

Let us assume that the frequency of the excitation force equals the natural frequency $\tilde{\omega}_J$ of the Jth mode of the structure, i.e.

$$\bar{F}^J = \hat{F}\,\mathrm{e}^{\mathrm{j}\tilde{\omega}_J t}, \quad \tilde{\omega}_J = \sqrt{\tilde{K}^J \big/ \tilde{M}^J}. \tag{A.3}$$

Since the system is linear, the dynamic response represented by the generalised coordinate q^J takes the form

$$q^J = Q^J\,\mathrm{e}^{\mathrm{j}\tilde{\omega}_J t}, \tag{A.4}$$

which, when substituted into Eq. (A.2), gives that

$$-\tilde{\omega}_J^2\tilde{M}^J Q^J + \mathrm{j}\zeta\tilde{K}^J Q^J + \tilde{K}^J Q^J = \hat{F}^J. \tag{A.5}$$

Eq. (A.5) describes the vibration of the structure, with a hysteretic damping represented by the complex elastic tensor $E^*_{ijkl} = (1+\mathrm{j}\eta)E_{ijkl}$, in the Jth natural frequency and the corresponding mode.

In vibration analysis [26,28–30], a viscous damping model is often used. Information on the viscous damping of the material of a structure is rarely, if ever known, and therefore, in an engineering analysis, an equivalent viscous damping coefficient [26] can be obtained as follows. Let the equivalent viscous damping coefficient of the Jth natural mode of the structure be represented by $\tilde{C}^J$. The vibration of the structure (with the equivalent viscous damping) in the Jth natural frequency and associated mode can be derived using a similar approach to the one adopted to derive Eq. (A.1). Following such a procedure, we find that Eq. (A.5) for the case incorporating the equivalent viscous damping coefficient $\tilde{C}^J$ is obtained as

$$-\tilde{\omega}_J^2\tilde{M}^J Q^J + \mathrm{j}\tilde{\omega}_J\tilde{C}^J Q^J + \tilde{K}^J Q^J = \hat{F}^J. \tag{A.6}$$

A comparison of Eqs. (A.5) and (A.6) gives the equivalent viscous damping coefficient $\tilde{C}^J$ of the Jth natural mode of the structure as

$$\tilde{C}^J = \frac{\zeta\tilde{K}^J}{\tilde{\omega}_J}. \tag{A.7}$$

As often used in vibration analysis [26,28–30], the normalised natural mode is chosen so that a unit generalised mass $\tilde{M}^J = 1$ in Eq. (20) is obtained. From Eqs. (A.3) and (A.7), it follows that

$$\tilde{K}^J = \tilde{\omega}_J^2, \quad \tilde{C}^J = \zeta\tilde{\omega}_J. \tag{A.8}$$

Therefore, for a uniform isotropic material with a hysteretic damping factor ζ, the corresponding equivalent viscous damping coefficient $\tilde{C}^J$ is proportional to the natural frequency $\tilde{\omega}^J$.

Furthermore, to understand this equivalent viscous damping, we need to calculate the energy dissipated in a vibration cycle by damping. The generalised coordinate in Eq. (A.4) is rewritten as

$$q^J = |Q^J|\,\mathrm{e}^{\mathrm{j}(\tilde{\omega}_J t-\varphi)}, \tag{A.9}$$

where $|Q^J|$ and φ represent the real amplitude and real phase angle of the generalised coordinate q^J. The damping force associated with the hysteretic damping defined in Eq. (A.2) is given by

$$F_h = \mathrm{j}\zeta\tilde{K}^J q^J = \mathrm{j}\zeta\tilde{K}^J |Q^J| \, \mathrm{e}^{\mathrm{j}(\tilde{\omega}_J t-\varphi)}. \tag{A.10}$$

The energy dissipated in a vibration cycle by hysteretic damping is calculated as follows:

$$\begin{aligned} W_h &= \int_0^{2\pi/\tilde{\omega}_J} \mathrm{Re}\{F_h\} \, \mathrm{d}(\mathrm{Re}\{q^J\}) \\ &= \int_0^{2\pi/\tilde{\omega}_J} \zeta\tilde{\omega}_J\tilde{K}^J |Q^J|^2 \sin^2(\omega_J t-\varphi) \, \mathrm{d}t = \zeta\pi\tilde{K}^J |Q^J|^2. \end{aligned} \tag{A.11}$$

Here, $\mathrm{Re}\{x\}$ denotes the real part of a complex variable x. In a similar approach using Eqs. (A.6) and (A.9), we obtain the equivalent viscous damping force and its dissipation of energy as given by

$$F_v = \mathrm{j}\tilde{\omega}_J\tilde{C}^J |Q^J| \, \mathrm{e}^{\mathrm{j}(\tilde{\omega}_J t-\varphi)}, \tag{A.12}$$

$$\begin{aligned} W_v &= \int_0^{2\pi/\tilde{\omega}_J} \mathrm{Re}\{F_v\} \, \mathrm{d}(\mathrm{Re}\{q^J\}) \\ &= \int_0^{2\pi/\tilde{\omega}_J} \tilde{\omega}_J^2\tilde{C}^J |Q^J|^2 \sin^2(\omega_J t-\varphi) \, \mathrm{d}t = \pi\tilde{\omega}_J\tilde{C}^J |Q^J|^2. \end{aligned} \tag{A.13}$$

By equality of energy dissipated in a vibration cycle by hysteretic and equivalent viscous damping, i.e. $W_h = W_v$, we derive Eq. (A.7). Therefore, physically, the equivalent viscous damping coefficient $\tilde{C}^J$ represented by Eq. (A.7) has a specific representation. That is, any non-viscous damping can be idealised by an equivalent viscous damping which dissipates the same amount of energy per vibration cycle. The introduction of an equivalent viscous damping allows use of the well-developed vibration analysis theory [28,29], based on a viscous damping assumption, to study the vibration of a system with non-viscous damping. This approach in association with vibration tests has often been used to model the damping of a complex system. In vibration experiments [15], it was shown that measurements of the energy dissipated in a vibration cycle of the system by damping allowed determination of its equivalent viscous damping coefficient.

Appendix B

A practical engineering structure (such as an airplane, car, building or a 3-D dam, etc.), is a composite body consisting of many types of structures. Eqs. (1)–(4) cover the corresponding equations describing the dynamics of each type of structure. To explain this, we represent the displacement, strain and stress of the structure in the column vectors $\mathbf{u}$, $\boldsymbol{\varepsilon}$ and $\boldsymbol{\sigma}$ under a coordinate system $o{-}xyz$ ($x = x_1$, $y = x_2$, $z = x_3$), respectively. For different types of structures used in engineering, these vectors are listed in Table B1. Based on these notations,

Table B1
Corresponding kinematic and static variables in various problems

Problem	Displacement vector $\mathbf{u}^{\mathrm{T}}$	Strain vector $\boldsymbol{\varepsilon}^{\mathrm{T}}$	Stress vector $\boldsymbol{\sigma}^{\mathrm{T}}$
Bar	u	ε_{xx}	σ_{xx}
Beam	w	κ_{xx}	M_{xx}
Plane stress	u, v	ε_{xx}, ε_{yy}, ε_{xy}	σ_{xx}, σ_{yy}, σ_{xy}
Plane strain	u, v	ε_{xx}, ε_{yy}, ε_{xy}	σ_{xx}, σ_{yy}, σ_{xy}
Axisymmetric	u, v	ε_{xx}, ε_{yy}, ε_{xy}, ε_{zz}	σ_{xx}, σ_{yy}, σ_{xy}, σ_{zz}
Three-dimensional	u, v, w	ε_{xx}, ε_{yy}, ε_{zz}, ε_{xy}, ε_{yz}, ε_{zx}	σ_{xx}, σ_{yy}, σ_{zz}, σ_{xy}, σ_{yz}, σ_{zx}
Plate bending	w	κ_{xx}, κ_{yy}, κ_{xy}	M_{xx}, M_{yy}, M_{xy}

the governing Eqs. (1)–(4) are rewritten in an equivalent matrix form

$$\mathbf{D}^{\mathrm{T}}\boldsymbol{\sigma} = \rho\mathbf{u}_{,tt} + \sum_{\alpha=1}^{n} \hat{\hat{f}}_{\alpha}(\mathbf{x}, \mathbf{x}^{\alpha})\boldsymbol{\gamma}^{\alpha}, \quad \mathbf{x} \in V, \tag{B.1}$$

$$\boldsymbol{\sigma} = (1 + \mathrm{j}\zeta)\mathbf{E}\,\boldsymbol{\varepsilon}, \quad \mathbf{x} \in V, \tag{B.2}$$

$$\boldsymbol{\varepsilon} = \mathbf{D}\mathbf{u}, \quad \mathbf{x} \in V, \tag{B.3}$$

$$\begin{cases} \boldsymbol{\nu}^{\mathrm{T}}\boldsymbol{\sigma} = 0, & \mathbf{x} \in S_T, \\ \mathbf{d}^{\mathrm{T}}\mathbf{u} = 0, & \mathbf{x} \in S_u. \end{cases} \tag{B.4}$$

Here, $\mathbf{E}$ denotes an stress–strain matrix involving Young's modulus E and Poisson's ratio μ of the materials of structures, $\mathbf{D}$ and $\mathbf{d}$ represent two differential operator matrices and $\boldsymbol{\nu}$ is another operator matrix relating to a unit normal vector $[v_x \quad v_y \quad v_z]^{\mathrm{T}}$ on the force boundary of the body. These matrices corresponding to different types of problems are given in Table B2 and B3. The set of equations defining the natural vibration of the system (no damping and external forces) is obtained when the stress and strain are eliminated from Eqs. (B.1)–(B.4). That is

$$\begin{aligned} &\mathbf{D}^{\mathrm{T}}\mathbf{E}\mathbf{D}\mathbf{u} = \rho\mathbf{u}_{,tt}, \quad \mathbf{x} \in V, \\ &\boldsymbol{\nu}^{\mathrm{T}}\mathbf{E}\mathbf{D}\mathbf{u} = 0, \quad \mathbf{x} \in S_T, \\ &\mathbf{d}^{\mathrm{T}}\mathbf{u} = 0, \quad \mathbf{x} \in S_u. \end{aligned} \tag{B.5}$$

The solutions of this set of equations define the natural frequencies and modes of the system. For complex engineering structures consisting of many different types of structural members, there are no available theoretical solutions of Eq. (B.5). A numerical approach has to be used to solve the problem. The powerful finite element method and well-developed computer software may be the best choice to complete the eigenvalue analysis defined by Eq. (B.5). Based on the obtained natural frequencies and modes, the developed

Table B2
Corresponding matrices $\mathbf{D}$, $\boldsymbol{\nu}$ and $\mathbf{d}$ in various problems

Problem	Matrix $\mathbf{D}$	Matrix $\boldsymbol{\nu}$	Matrix $\mathbf{d}$
Bar	$[\partial/\partial x]$	$[v_x]$	1
Beam	$[\partial^2/\partial x^2]$	$[1 \quad \partial/\partial x]$	$[1 \quad \partial/\partial x]$
Plane stress & strain	$\begin{bmatrix} \partial/\partial x & 0 \\ 0 & \partial/\partial y \\ \partial/\partial y & \partial/\partial x \end{bmatrix}$	$\begin{bmatrix} v_x & 0 \\ 0 & v_y \\ v_y & v_x \end{bmatrix}$	$\begin{bmatrix} 1 & 0 \\ 0 & 1 \end{bmatrix}$
Axisymmetric	$\begin{bmatrix} \partial/\partial x & 0 \\ 0 & \partial/\partial y \\ \partial/\partial y & \partial/\partial x \\ 1/x & 0 \end{bmatrix}$	$\begin{bmatrix} v_x & 0 & 0 \\ 0 & v_y & 0 \\ v_y & v_x & 0 \\ 0 & 0 & v_z \end{bmatrix}$	$\begin{bmatrix} 1 & 0 \\ 0 & 1 \end{bmatrix}$
Three-dimensional	$\begin{bmatrix} \partial/\partial x & 0 & 0 \\ 0 & \partial/\partial y & 0 \\ 0 & 0 & \partial/\partial z \\ \partial/\partial y & \partial/\partial x & 0 \\ 0 & \partial/\partial z & \partial/\partial y \\ \partial/\partial z & 0 & \partial/\partial x \end{bmatrix}$	$\begin{bmatrix} v_x & 0 & 0 \\ 0 & v_y & 0 \\ 0 & 0 & v_z \\ v_y & v_x & 0 \\ 0 & v_z & v_y \\ v_z & 0 & v_x \end{bmatrix}$	$\begin{bmatrix} 1 & 0 & 0 \\ 0 & 1 & 0 \\ 0 & 0 & 1 \end{bmatrix}$
Plate bending	$\begin{bmatrix} \partial^2/\partial x^2 \\ \partial^2/\partial y^2 \\ 2\partial^2/\partial x\,\partial y \end{bmatrix}$	$\begin{bmatrix} 1 & 0 & 0 & \partial/\partial x & 0 \\ 0 & 1 & 0 & 0 & \partial/\partial y \\ 0 & 0 & 1 & \partial/\partial y & \partial/\partial x \end{bmatrix}$	$[1 \quad \partial/\partial x \quad \partial/\partial y]$

Table B3
Stress–strain matrices for isotropic materials and the problems in Table B1

Problem	Stress–strain matrix **E**
Bar	E
Beam	EI
Plane stress	$\dfrac{E}{(1-\mu^2)}\begin{bmatrix} 1 & \mu & 0 \\ \mu & 1 & 0 \\ 0 & 0 & \dfrac{1-\mu}{2} \end{bmatrix}$
Plane strain	$\dfrac{E(1-\mu)}{(1+\mu)(1-2\mu)}\begin{bmatrix} 1 & \bar{\mu} & 0 \\ \bar{\mu} & 1 & 0 \\ 0 & 0 & \hat{\mu} \end{bmatrix}$
Axisymmetric	$\dfrac{E(1-\mu)}{(1+\mu)(1-2\mu)}\begin{bmatrix} 1 & \bar{\mu} & 0 & \bar{\mu} \\ \bar{\mu} & 1 & 0 & \bar{\mu} \\ 0 & 0 & \hat{\mu} & 0 \\ \bar{\mu} & \bar{\mu} & 0 & 1 \end{bmatrix}$
Three-dimensional	$\dfrac{E(1-\mu)}{(1+\mu)(1-2\mu)}\begin{bmatrix} 1 & \bar{\mu} & \bar{\mu} & 0 & 0 & 0 \\ \bar{\mu} & 1 & \bar{\mu} & 0 & 0 & 0 \\ \bar{\mu} & \bar{\mu} & 1 & 0 & 0 & 0 \\ 0 & 0 & 0 & \hat{\mu} & 0 & 0 \\ 0 & 0 & 0 & 0 & \hat{\mu} & 0 \\ 0 & 0 & 0 & 0 & 0 & \hat{\mu} \end{bmatrix}$
Plate bending	$\dfrac{Eh^3}{12(1-\mu^2)}\begin{bmatrix} 1 & \mu & 0 \\ \mu & 1 & 0 \\ 0 & 0 & \dfrac{1-\mu}{2} \end{bmatrix}$

$\bar{\mu} = \mu/(1-\mu)$, $\hat{\mu} = (1-2\mu)/(2(1-\mu))$, h = thickness of plate, I = moment of inertia.

formulations in this paper can be used to investigate the structure–control interactions. In this paper, we aim to provide the generalised theory and the related physical concepts on vibration structure–control interactions. Therefore, the simple examples are used to explain the important concepts. The interested reader may follow the formulations described in this paper to create a computer software for generalised vibration structure–control analysis.

References

[1] G.W. Housner, L.A. Bergman, T.K. Caughey, A.G. Chassiakos, R.O. Claus, S.F. Masri, R.E. Skelton, T.T. Soong, B.F. Spencer, J.T.P. Yao, Structural control: past, present, and future, *Journal of Engineering Mechanics* 123 (1997) 897–971.

[2] C.R. Fuller, S.J. Elliott, P.A. Nelson, *Active Control of Vibration*, Academic Press, London, 1996.

[3] S.J. Elliott, *Signal Processing for Active Control*, Academic Press, London, 2001.

[4] T.W. Lim, P.A. Cooper, J.K. Ayers, Structural dynamic interaction with solar tracking control for evolutionary space station concepts, *Proceedings of the 33rd Structures, Structural Dynamics and Materials Conference*, Dallas, TX, 13–15 March 1992.

[5] J.K. Cheng, G.D. Ianculescu, C.S. Kenney, A. Laub, J. Ly, H.Q. Jason, P.M. Papadopoulos, Control–structure interaction, *IEEE Control Systems Magazine* 12 (1992) 4–13.

[6] R.D. Quinn, I.S. Yunis, Control/structure interactions of space station solar dynamic modules, *Journal of Guidance, Control, and Dynamics* 16 (1993) 623–629.

[7] M. Subramaniam, K.W. Byun, T. Hua, Control structure interaction analysis of the International Space Station, *Seventh AIAA/USAF/NASA/ISSMO Symposium on Multidisciplinary Analysis and Optimization*, St. Louis, MO, September 2–4, 1998, Collection of Technical Papers, part 3 (A98-39701 10-31), AIAA-1998-4924.

[8] D.S. Chang, J.F. Lee, Flexible space station attitude control system analysis and design, *AIAA Guidance, Navigation and Control Conference*, Hilton Head Island, SC, August 10–12, 1992, Technical Papers, part 2 (A92-55151 23-63).

[9] J.A. Schliesing, L.S. Shieh, Controls–structures-interaction dynamics during RCS control of the orbiter/SRMS/SSF configuration, *The Fifth NASA/DOD Controls–Structures Interaction Technology Conference*, part 2 (SEE N93-18928 06-18), NASA. Langley Research Center, 1993, pp. 509–527.
[10] S.E. Morgan, Avoiding on-orbit control/structure interaction problems with space station freedom SAE, *Aerotech '92 Conference*, Anaheim, CA, October 5–8, 1992, p. 10.
[11] D.S. Chang, J.B. Caldwell, Control–structure interaction of multi-flexible-body space station and RCS attitude control SAE, *Aerotech '92 Conference*, Anaheim, CA, October 5–8, 1992, p. 12.
[12] V.J. Modi, A. Suleman, Control–structure interaction study of the proposed space station freedom IAF, *43rd International Astronautical Congress*, Washington, August 28–September 5, 1992, p. 13.
[13] S.J. Dyke, B.F. Spencer, P. Quast, M.K. Sain, Role of control–structure interaction in protective system design, *Journal of Engineering Mechanics* 121 (1995) 322–338.
[14] J.B. Mohl, H.W. Davis, C-SIDE: the control–structure interaction demonstration experiment, *The Fifth NASA/DOD Controls–Structures Interaction Technology Conference*, part 2 (SEE N93-18928 06-18), NASA, Langley Research Center, 1993, pp. 455–474.
[15] J.T. Xing, *Theory and Techniques on Mode Vibration Experiments of Aircraft Structures, Lecture Notes*, NAI Press, Nanjing, China, 1975 (in Chinese).
[16] J.W. Umland, Active Damping Using a Control–Structure Interaction Approach, PhD Thesis, State University of New York, Buffalo, 1991.
[17] C.C. Won, Vibration control–structure interaction in adaptive structures, *Proceedings of SEM Spring Conference on Experimental Mechanics*, Milwaukee, WI, June 10–13, 1991 (A93-16601 04-39), pp. 485–492.
[18] S.J. Elliot, L. Benassi, M.J. Brennan, P. Gardonio, X. Huang, Mobility analysis of active isolation systems, *Journal of Sound and Vibration* 271 (2004) 297–321.
[19] L. Benassi, S.J. Elliot, P. Gardonio, Active vibration isolation using an in inertial actuator with local force feedback control, *Journal of Sound and Vibration* 278 (2004) 705–724.
[20] J.T. Xing, Y.P. Xiong, W.G. Price, Passive–active vibration isolation systems with zero or infinite dynamic modulus: theoretical and conceptual design strategies, *Journal of Sound and Vibration* 286 (2005) 615–636.
[21] Y.P. Xiong, J.T. Xing, W.G. Price, A general linear mathematical model of power flow analysis and control for integrated structure–control systems, *Journal of Sound and Vibration* 267 (2003) 301–334.
[22] R. Alkhatib, M.F. Golnaraghi, Active structural vibration control: a review, *Shock and Vibration Digest* 35 (2003) 367–383.
[23] Cerny, A confirmation to modal analysis experimental procedures of aircraft flight control non-linear systems, Report VZLU ED Documentation No. 67/2230/98, 1998.
[24] Cerny, V. Hlavaty, A ground vibration test of the L-610G type aircraft, Report VZLU Z-3667/98, 1998.
[25] Y.C. Fung, *A First Course in Continuum Mechanics*, Prentice-Hall, Englewood Cliffs, NJ, 1977.
[26] C.G. Harris, C.E. Crede, *Shock and Vibration Handbook*, second ed., McGraw-Hill, Inc., New York, 1976.
[27] C. Kittel, *Berkeley Physics Course*, McGraw-Hill, New York, 1967.
[28] R.E.D. Bishop, D.C. Johnson, *The Mechanics of Vibration*, Cambridge University Press, Cambridge, 1979.
[29] R.E.D. Bishop, G.M.L. Gladwell, S. Michaelson, *The Matrix Analysis of Vibration*, Cambridge University Press, Cambridge, 1965.
[30] W.T. Thomson, *Theory of Vibration with Applications*, third ed., Prentice-Hall, London, 1988.
[31] R. Courant, D. Hilbert, *Methods of Mathematical Physics*, Interscience Publishers, New York, 1953.
[32] A. Hurwitz, On the condition under which an equation has only roots with negative real part, in: R. Bellman, R. Kalaba (Eds.), *Selected Papers on Mathematical Trends in Control Theory*, Dover, New York, 1964, pp. 72–82.